AD-A115 719 NAVAL POSTGRADUATE SCHOOL MONTEREY CA F/G 20/1
FINITE-AMPLITUDE STANDING WAVES IN A CAVITY WITH BOUNDARY PERTU--ETC(U)
APR 82 A B COPPENS, J V SANDERS, I JOUNG
UNCLASSIFIED NPS61-82-005 NL

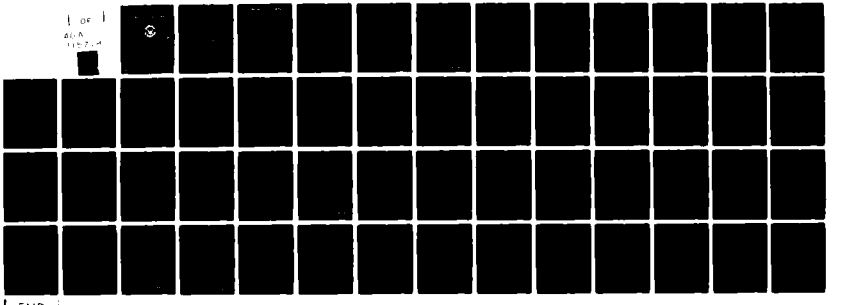

END
DATE FILMED
07-82
DTIC

(2)

NPS61-82-005

NAVAL POSTGRADUATE SCHOOL

Monterey, California

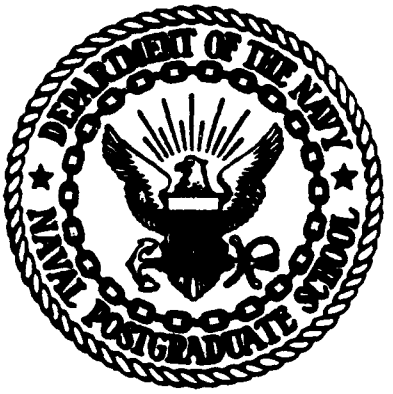

FINITE-AMPLITUDE STANDING WAVES
IN A CAVITY WITH BOUNDARY PERTURBATIONS

BY

A.B. Coppens, J.V. Sanders and I. Joung

Naval Postgraduate School
Monterey, CA 93940

April 1982

Prepared for:
Chief of Naval Research
ATTN: Dr. Logan Hargrove
800 Quinch Street
Arlington, VA 22217

NAVAL POSTGRADUATE SCHOOL
Monterey, California

Rear Admiral J. J. Ekelund
Superintendent

D. A. Schrady
Acting Provost

The work reported herein was supported in part by the Office of Naaval Research, Washington, D.C.

This report was prepared by:

A.B. COPPENS
Professor of Physics

J.V. SANDERS
Professor of Physics

Approved by:

J. N. DYER, Chairman
Department of Physics

William M. Tolles
Dean of Research

UNCLASSIFIED

SECURITY CLASSIFICATION OF THIS PAGE (When Data Entered)

REPORT DOCUMENTATION PAGE		READ INSTRUCTIONS BEFORE COMPLETING FORM
1. REPORT NUMBER 61-82-005	2. GOVT ACCESSION NO. AD-A115 719	3. RECIPIENT'S CATALOG NUMBER
4. TITLE (and Subtitle) Finite-Amplitude Standing Waves in a Cavity With Boundary Perturbations		5. TYPE OF REPORT & PERIOD COVERED Technical Report 6. PERFORMING ORG. REPORT NUMBER
7. AUTHOR(s) A.B. Coppens, J.V. Sanders and I. Joung		8. CONTRACT OR GRANT NUMBER(s)
9. PERFORMING ORGANIZATION NAME AND ADDRESS Naval Postgraduate School Monterey, CA 93940		10. PROGRAM ELEMENT, PROJECT, TASK AREA & WORK UNIT NUMBERS 61153n; RR032-01-01 N0001481WR10171
11. CONTROLLING OFFICE NAME AND ADDRESS Chief of Naval Research ONR 800 Quincy St. ATTN: Dr. Logan Hargrove Arlington, VA 22217		12. REPORT DATE April 1982 13. NUMBER OF PAGES 50
14. MONITORING AGENCY NAME & ADDRESS(if different from Controlling Office)		15. SECURITY CLASS. (of this report) unclassified 15a. DECLASSIFICATION/DOWNGRADING SCHEDULE

16. DISTRIBUTION STATEMENT (of this Report)

Approved for public release; distribution unlimited

17. DISTRIBUTION STATEMENT (of the abstract entered in Block 20, if different from Report)

18. SUPPLEMENTARY NOTES

19. KEY WORDS (Continue on reverse side if necessary and identify by block number)

Finite amplitude acoustics
Standing Waves
Rectangular Cavity
Boundary Perturbation

20. ABSTRACT (Continue on reverse side if necessary and identify by block number)

Finite amplitude acoustic standing waves in a rectangular air-filled cavity with various wedge-shape boundary perturbations were studied both experimentally and theoretically. The experimental results show that geometrical perturbations alter the finite-amplitude behavior of the cavity and that the nature of these changes are in qualitative agreement with the predictions of the theory. However, quantitative agreement was not observed,

DD FORM 1 JAN 73 1473 EDITION OF 1 NOV 65 IS OBSOLETE
S/N 0102-014-6601

UNCLASSIFIED

SECURITY CLASSIFICATION OF THIS PAGE (When Data Entered)

possibly because the perturbation chosen did not satisfy all the assumptions of theory.

ABSTRACT

Finite amplitude acoustic standing waves in a rectangular air-filled cavity with various wedge-shape boundary perturbations were studied both experimentally and theoretically. The experimental results show that geometrical perturbations alter the finite-amplitude behavior of the cavity and that the nature of these changes are in qualitative agreement with the predictions of the theory. However, quantitative agreement was not observed, possibly because the perturbation chosen did not satisfy all the assumptions of theory.

TABLE OF CONTENTS

I. INTRODUCTION

Coppens and Sanders [1,2] developed a non-linear acoustic model with the dissipative term phenomonologically describing the viscous and thermal energy losses actually encountered at the walls of a rectangular rigid cavity. Several researchers [3,4] have examined the problems and experimental results are in excellent agreement with the theory except when a degeneracy exists in the cavity.

The purpose of this research was to examine the finite-amplitude behavior within a cavity for which perturbation effects can be accurately measured and to compare the results with the predictions of the model.

II. BACKGROUND AND THEORY

In 1975 Coppens and Sanders [2] formulated a perturbation expansion for the non-linear acoustic wave equation with a dissipative term describing the measured absorption properties and the measured resonance frequencies for standing waves within a real, fluid filled, rigid-walled cavity. This model predicts that, when a near-degeneracy exists, geometrical perturbations provide a mechanism whereby a nearly degenerate mode can affect the finite-amplitude behavior of the cavity.

The non-linear wave equation of the viscous fluid [2] is,

$$(c_o^2\Box^2+\partial\mathcal{L}/\partial t)\ p/\rho_o c_o^2=\partial^2/\partial t^2[(u/c_o)^2+\tfrac{1}{2}(\gamma-1)(p/\rho_o c_o^2)^2] \qquad (1)$$

where $c_o^2 = (\partial p/\partial\rho)$ (adiabatic), ρ_o is the equilibrium density of the fluid, p the acoustic pressure, u the magnitude of the acoustic velocity, γ the ratio of heat capacities, and $\mathcal{L}$ an operator describing the physical processes for absorption and dispersion. The term on the right can be interpreted as a distribution of virtual sources created by the self-interaction of the standing waves.

Pressure standing waves in a rectangular cavity of dimension L_x, L_y, L_z have the form

$$p \quad \cos k_x x \cos k_y y \cos k_z z \cos \omega t$$

where

$$k_x = j\pi/L_x \qquad j = 0,1,2,\ldots$$

$$k_y = \ell\pi/L_y \qquad \ell = 0,1,2,\ldots$$

$$k_z = m\pi/L_z \qquad m = 0,1,2,\ldots$$

and $j+\ell+m\neq 0$

If the cavity is being driven near resonance, the contributions of non-resonant terms are negligible with respect to the resonant terms; the acoustic field has the form

$$p = \sum_{n=0}^{\infty} p_n \tag{2}$$

where

$$p_n/\rho_o c_o^2 = MR_n \cos n k_x x \cos n k_y y \cos n k_z z \sin(n\omega t + \phi_n)$$

M is the Mach number $|u/c_o|$, $R_1=1$, and R_n is the relative amplitude of the n-th standing wave. By substituting (2) into (1), a set of coupled, non-linear, transcendental equations is obtained,

$$R_n \begin{Bmatrix}\cos\\ \sin\end{Bmatrix}(\phi_n-\theta_n) = NMBQ_n \cos\theta_n \left[\tfrac{1}{2} \sum_{j=1}^{n-1} R_j R_{n-j} \begin{Bmatrix}\cos\\ \sin\end{Bmatrix}(\phi_j-\phi_{n-j}) - \sum_{j=1}^{\infty} R_{n+j} R_j \begin{Bmatrix}\cos\\ \sin\end{Bmatrix}(\phi_{n+j}-\phi_j) \right] \tag{3}$$

where N = 1 for axial, 2 for tangential, and 3 for oblique standing waves.

If a geometrically-perfect rectangular cavity is driven at frequencies near the resonance frequency of the (0,1,0) standing wave, only the <u>family members</u> (0,n,0) will contribute significantly to the finite amplitude behavior.

In this research we were interested in this behavior when a degeneracy exists between the (0,2,0) and (1,0,0) modes and the cavity is not a perfect right parallelepiped.

If we define a <u>perturbation parameter</u> ε as a dimensionless measure of the magnitude of any irregularities on the cavity

surfaces compared to the effective dimensions of the cavity, the effect of the perturbation on the standing wave p_n that would exist in the ideal cavity can be expressed as a small correction p' so that the true pressure field p_n' is

$$p_n' = p_n + \varepsilon p'$$

For the case of interest, n denotes the (0,2,0) standing wave and p' is the perturbation-generated (1,0,0) standing wave of nearly identical resonance frequency.

III. SAMPLE CALCULATION OF THE PRESSURE DISTRIBUTION WITH A WEDGE PERTURBATION

The pressure distribution of the (0,2,0) wave has the form

$$p_2 = P \cos(2\pi y/L_y) \cos(2\omega t+\theta_2) \tag{1}$$

where P and θ_2 are constant determined by the driving conditions.

For this example, let the equation for the perturbed boundary (Fig. 0) be

$$x = L_x \{1-(\Delta/L_x)\ [(4/L_y)(y-3L_y/4)][U(y-3L_y/4)-U(y-L_y)]\}$$

$$= L_x\ [1+\epsilon f(y,z)] \tag{2}$$

where

$$\epsilon \equiv \Delta/L_x$$

$$f(y,z) = -(4/L_y)(y-3L_y/4)\,[U(y-3L_y/4)-U(y-L_y)]$$

$$U(y) = \begin{cases} 0 \text{ if } y < 0 \\ 1 \text{ if } y > 0 \end{cases}$$

Differentiating p_2 and $f(y,z)$ with respect to y gives

$$\partial p_2/\partial y = -(2\pi P/L_y)\ \sin(2\pi y/L_y)\ \cos(2\omega t+\theta_2)$$

and

$$\partial f/\partial y = -(4/L_y)\,[U(y-3L_y/4)-U(y-L_y)]$$

$$-(4/L_y)\,(y-3L_y/4)\,[\delta(y-3L_y/4)-\delta(y-L_y)] \qquad (3)$$

and $\delta(y)$ is the Dirac delta function.

Now, it can be shown by standard perturbation analysis [4] that the perturbation correction p' must satisfy the boundary condition

$$(\partial p'/\partial_x)_{L_x} = L_x(\partial f/\partial y)(\partial p_2/\partial y)_{L_x}$$

Substituting, we obtain

$$(\partial p'/\partial x)_{L_x} = A\ \sin(2\pi y/L_y)\ \cos(2\omega t+\theta_2)\{U(y-3L_y/4)-U(y-L_y)$$

$$+\ (y-3L_y/4)\,[\delta(y-3L_y/4)-\delta(y-L_y)]\} \qquad (4)$$

where

$$A = 8\pi PL_x/L_y^{\,2}$$

Equation (4) can be expanded as a Fourier series,

$$(\partial p'/\partial x)_{L_x} = A\ \cos(2\omega t+\theta_2)\ \sum_{m=0}^{\infty}\ [A_m\ \cos(m\pi y/L_y)+b_m\ \sin(m\pi y/L_y)] \qquad (5)$$

Only A_o is needed to determine the first order correction term due to the degeneracy between the (0,2,0) and (1,0,0) waves:

$$A_o = 1/2\pi$$

The perturbation correction p' is

$$p' = (Ac_o^2/\pi L_x 4\omega^2)\ Q_{100}\sin\tau_{100}\ \cos(\pi x/L_x)\cos(2\omega t+\theta_2+\tau_{100}) \qquad (6)$$

where the phase angle τ is given by

$$\tan\tau_{100} = Q_{100}[1-(f_{100}/2f)^2]$$

The pressure at the microphone position $x=L_x$ can be written as follows (with $2\omega/c_o \doteq 4\pi/L_y$),

$$p_{mic} = p_2 + \varepsilon p'$$

$$= P[\cos(2\omega t+\theta_2) + (\varepsilon/2\pi^2)\ Q_{100}\sin\tau_{100}\cos(2\omega t+\theta_2+\tau_{100})] \qquad (7)$$

The total pressure amplitude at the microphone will be

$$|p_{mic}| = P\sqrt{(1+B\cos\tau_{100})^2 + (B\sin\tau_{100})^2} \qquad (8)$$

where

$$B = (\varepsilon/2\pi^2)\ Q_{100}\sin\tau_{100} \qquad (9a)$$

B can also be expressed in terms of A_o for a wedge anywhere on the wall $x=L_x$ by

$$B = (\varepsilon A_o/\pi)\ Q_{100}\sin\tau_{100} \qquad (9b)$$

where A_o is calculated for any arbitrary position and wedge dimensions by the same method as developed above.

[In reference [5], the author made a error in formulating Equation (2); he used y instead of $(y-aL_x)$ and got an incorrect value of A_o.]

IV. DEFINITION OF SOME PARAMETERS

Several parameters will be defined for the purpose of simplifying the mathematical formulation and elucidating the physical content of the equations.

A. STRENGTH PARAMETERS: S

$$S = M\beta Q_1$$

where $\beta = (1/2)(1+\gamma)$ and Q_1 is the quality factor of the driven (0,1,0) standing wave. The strength parameter characterizes the strength of the finite-amplitude interaction. It is interesting to note that S is one half the Goldberg number. Since the microphone sensitivity S_m (obtained with a B&K 4220 pistonphone) is known,

$$S = M\beta Q_1 = 7.07 \times 10^{-3} V_1 Q_1$$

where

$M = \sqrt{2}\, V_1/\rho c_o^2 S_m$, $\beta = 1.2$ for air,

$\rho = 1.293$ kg/m^3, $c_o = 345$ m/s

V_1 = RMS output voltage of the first harmonic component, and

Q_1 is the quality factor of the driven (0,1,0) standing wave.

B. FREQUENCY PARAMETER: F_n

$$F_n(f) = Q_n[1-(f_n/f)^2]$$

where f is the driving frequency, and f_n and Q_n are the resonance frequency and quality factor for the (0,n,0) wave.

If $F_n<1$, the n^{th} harmonic of the driving frequency lies within the half-power frequencies of the resonance curve for the (0,n,0) wave.

For reasonably large values of Q_1,

$$F_1(f) \doteq 2 Q_1 (f-f_1)/f_1$$

C. HARMONICITY COEFFICIENT: E(n)

$$E(n) = (f_n - nf_1)/nf_1$$

E(n) characterizes how well the modes of a given family are tuned (harmonic). If $|E(n)| < 4$, the corresponding harmonic will be strongly excited.

V. APPARATUS

A. THE RECTANGULAR CAVITY

The cavity (Fig.1), constructed from 0.75-in. aluminum, has interior dimensions 12.00 in. long, 2.50 in. high, and a width that can be varied between 5.50 in. to 7.00 in. in 0.25 in. increments. All joints were sealed with a thin layer of silicon grease.

Figure 2 shows the pressure distribution for several of the lower modes of this cavity, and Table 0 presents the theoretical eigen frequencies calculated for a cavity 12 x 6 x 2.5 in. Note that the (0,2,0) and (1,0,0,) modes are predicted to be degenerate. Experimentally, the resonance frequency of the (0,2,0) standing wave was about 3 Hz higher than that of the (1,0,0) standing wave. The various configurations of wedge-perturbations are shown in Fig. 3.

The source piston is set flush with the bottom of the cavity as near to the wall y=0 as practical, and halfway between the wall at x=0 and x=L_x. In this position it can efficiently excite the (0,n,0) family of waves without appreciably exciting the (1,0,0) wave. To determine the proportion of the (1,0,0) mode, an auxilliary driver, an (ID-30), can be inserted at Position A.

A microphone at Position B will sense the pressure of all standing waves. If the microphone is placed at Position A, it senses the (1,0,0) wave with minimum contamination from the (0,2,0) wave and at Position C it senses the (0,2,0) wave with minimum contamination from the (1,0,0) wave.

B. APPARATUS

A block diagram of the apparatus is shown in Fig.4. A GR 1161-A coherent decade frequency synthesizer is used to produce a driving signal precise to within $\pm$0.001 Hz. This signal is applied to a 2120 MB power amplifier which, in turn, drives the shaker. The motion of the piston was continuously sensed by an Endevco Model 2215 Accelerometer mounted within the piston, and the output of the accelerometer was observed on a Model 130BR HP oscilloscope and measured on a HP 400D Voltmeter. A Schlumberger spectrum analyzer was used to measure the harmonic distortion in the piston motion.

The output of the B&K 1/4-in. microphone (with matching preamplifier B&K 2810) was fed into three devices; (1) an HP 400D VTVM to measure overall voltage level, (2) a Schlumberger spectrum analyzer to display the spectrum of the waveform, and (3) two HP 302A wave analyzers to measure the amplitudes of the first two harmonics of the pressure waveform.

VI. DATA COLLECTION PROCEDURE

Since the resonance frequencies of the cavity were observed to vary with time, the system was allowed to warm-up for at least one hour prior to data collection. The piston was then driven at the maximum amplitude to be expected during the run, and the harmonic content of the accelerometer output was analyzed and the piston was adjusted until the second harmonic of the accelerometer output was at least 50 dB below that of the fundamental. Figure 5 shows typical results for the percent second harmonic in the acceleration with the piston driven at a rather large amplitude. Finite-amplitude measurements were limited to those frequencies for which $V_2/V_1 < 0.01$.

There are three steps necessary for collecting accurate data; (1) pre-run infinitesimal-amplitude measurements, (2) finite-amplitude measurements, and (3) post-run infinitesimal-amplitude measurements.

A. PRE-RUN AND POST-RUN INFINITESIMAL-AMPLITUDE MEASUREMENTS

During these measurements, the piston was driven with the accelerometer output less than 0.1 V. Observation of spectra of the pressure waveforms obtained at these low amplitudes showed that the amplitudes of all overtones were at least 60 dB below that of the fundamental. The resonant frequencies f_n and the quality factors Q_n for the first few (0,n,0) waves were determined from

$$f_n = (f_u+f_\ell)/2$$

$$Q_n = f_n/(f_u-f_\ell)$$

where f_u and f_ℓ are the upper and lower half-power frequencies. The resonance frequency and Q of the (1,0,0) wave were determined by the same procedure but with the cavity driven at port A.

The harmonicity coefficients were then calculated from

$$E_n = (f_n-nf_1)/nf_1, \text{ for (0,n,0) wave}$$
$$= (f_{100}-f_2)/f_2, \text{ for the (1,0,0) wave}$$

where f_{100} is the resonance frequency of the (1,0,0) wave. The time at which each f_u and f_ℓ were taken was recorded.

B. THE FINITE AMPLITUDE MEASUREMENTS

Throughout this portion of the run, the strength parameter S was maintained constant by adjusting the driving voltage applied to the piston; with the microphone in Position B, the HP 302A wave analyzer was set to the driving frequency and the driving voltage adjusted to keep the amplitude of the fundamental of the pressure waveform V_1 constant as the frequency was changed. The frequency was increased 0.5 Hz steps through $\pm$6 Hz about the resonance frequency of the fundamental. At each driving frequency, the harmonic content of the microphone output (usually up to the fourth harmonic) was measured with the second HP 302A wave analyzer set on AFC mode. The time of each measurement was recorded.

To determine the frequency parameter at the time the harmonic content was measured, f_n at the instant of the measurement of V_n was estimated by interpolation of the f_n found in the pre- and post-run procedures. Figure 6 shows the drift in f_n is approximately linear in time. The results were presented as V_n/V_1 vs $F_1(f)$ for a given strength parameter and perturbation.

VII. RESULTS

The results are presented in graphical form in Appendix A and in tabular form in Appendix B.

Figure 7 shows the excellent agreement between theory and experiment obtained when there are no perturbations so that only one family of waves is excited. Some discrepancies were always observed when the driving frequency was far from the fundamental resonance frequency (for $|F_1| > 2$). In this region, the piston had to be driven hard to keep V_1 constant, causing significant second harmonic to appear in the piston waveform (as shown by Fig. 5), thereby introducing a linearly-generated second harmonic into the cavity.

For all cases studied, the pressure was calculated following the methodology of Sect. III.

For the boundary perturbation of Fig. 3, the results are plotted in Figs. 8 through 15. The thin line is the theoretical prediction in the absence of any perturbation and the thick line includes the perturbation correction. The circles are the experimental results. Along the edge of each figure is the information about the cavity configuration.

A. THE WEDGE AT THE CORNER OF THE CAVITY

Figures 8 through 11 show the results for a wedge at the corner of the cavity. The wedge used are those of Fig. 3(a)-(d) respectively.

B. THE WEDGE AT THE CENTER OF THE LONG WALL

Figures 12 through 15 show the results for the same wedges [Fig. 3(e)-(h)] but now located at the center of the long wall.

For Fig. 12 and 13, $A_o = 0.177$ with Δ for Fig. 13 twice that for Fig. 12. For Fig. 14 and 15, $A_o = 0.500$ with Δ the same as for Fig. 12 and 13.

VIII. CONCLUSIONS

A. The experimental apparatus and procedures are capable of providing data sufficiently precise to verify the prediction of the theory in the absence of geometrical perturbation if the range of driving frequencies is restricted so that the absolute value of the frequency parameter is less than 2.

B. To verify the correction for a geometrical perturbation, it is useful (1) to have a sufficiently large correction to the unperturbed prediction and (2) that the sign of the correction change for an absolute value of the frequency parameter less than 2.

C. The experimental results show that geometrical perturbation alters the finite amplitude behavior of the cavity, and that the nature these changes are in qualitative agreement with the predictions of the theory. However, quantitative agreement was ɔt observed.

D. Sources of the difficulties in obtaining good agreement might be (1) the inability to experimentally satisfy conditions of B above, and (2) the higher order terms neglected in developing the theory may not all be small. For example, terms of order higher than first order in Eq. (4) of Sect. II and terms of order higher than A_0 and all b_m in Eq. (5) of Sect. IV.

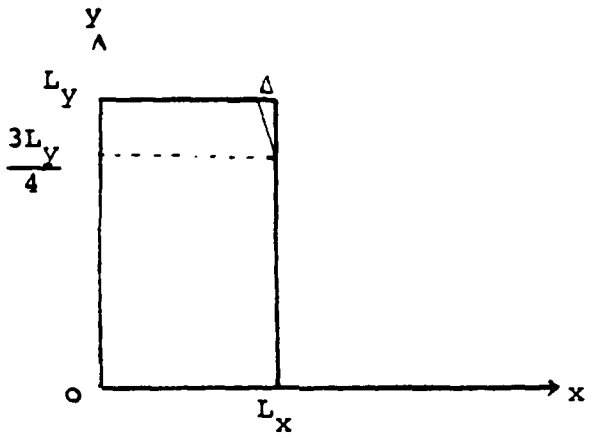

Fig. 0. Geometry of the wedge perturbation.

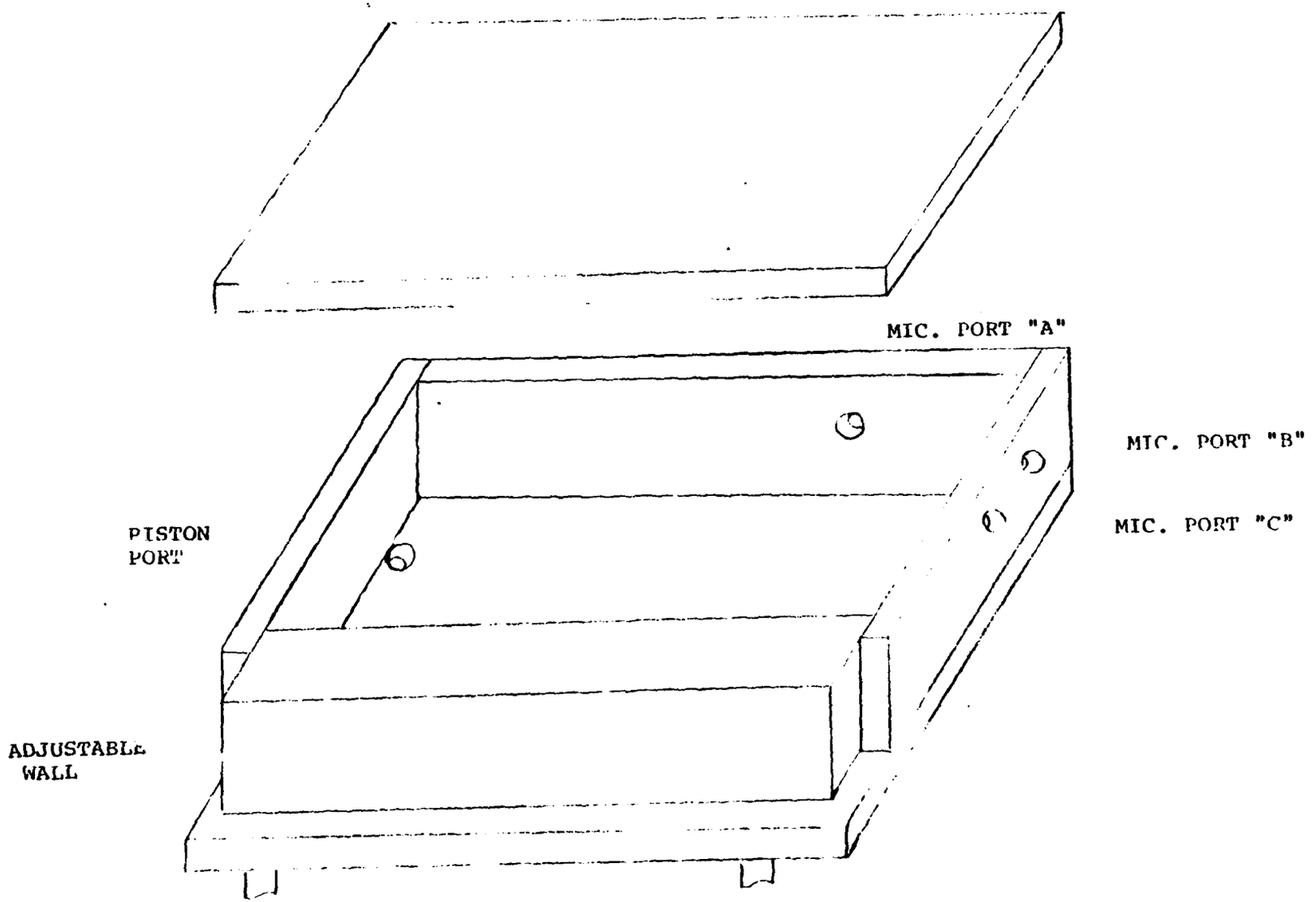

Fig. 1. Adjustable Rectangular Cavity

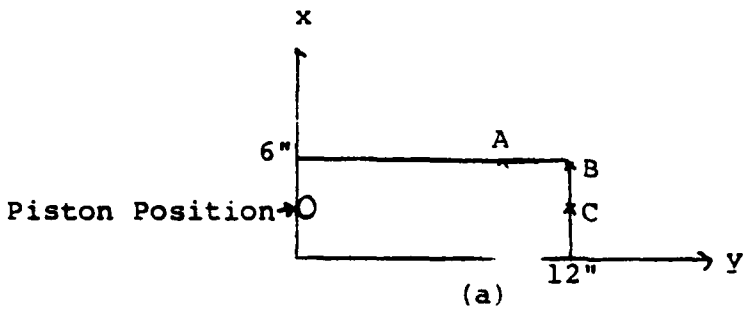

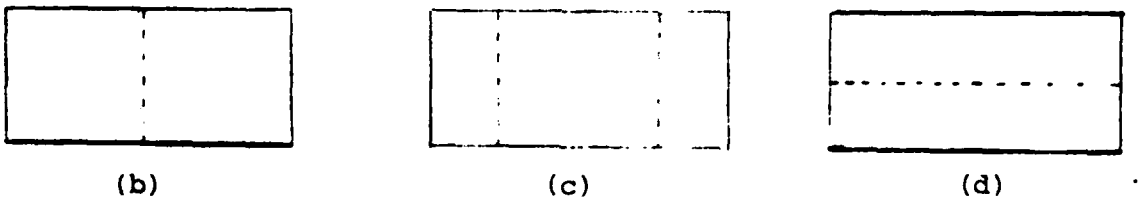

Fig. 2. (a) Cavity Orientation, (b) Pressure Nodes for (0,1,0), (c) For (0,2,0), (d) For (1,0,0).

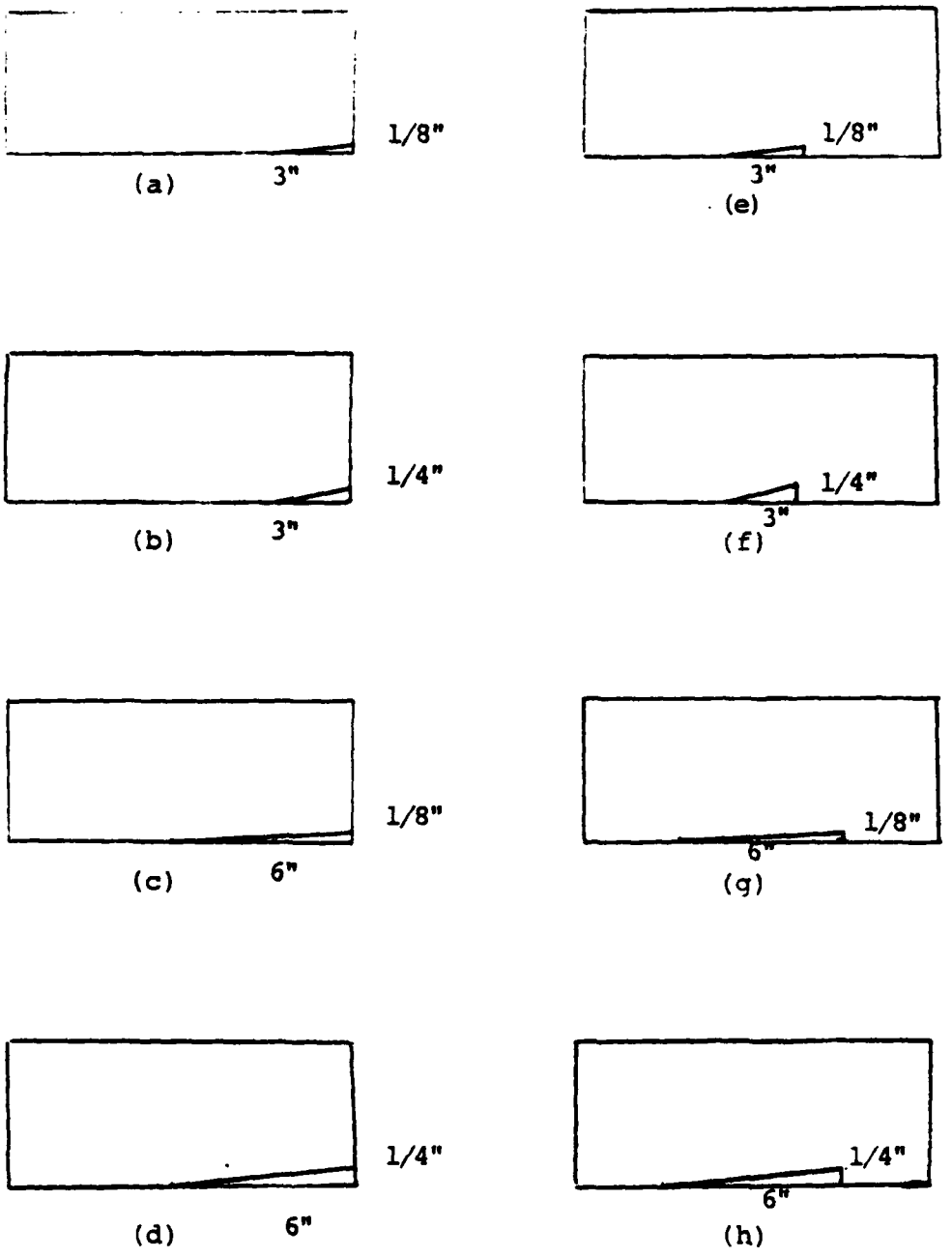

Fig. 3. Perturbation Configuration

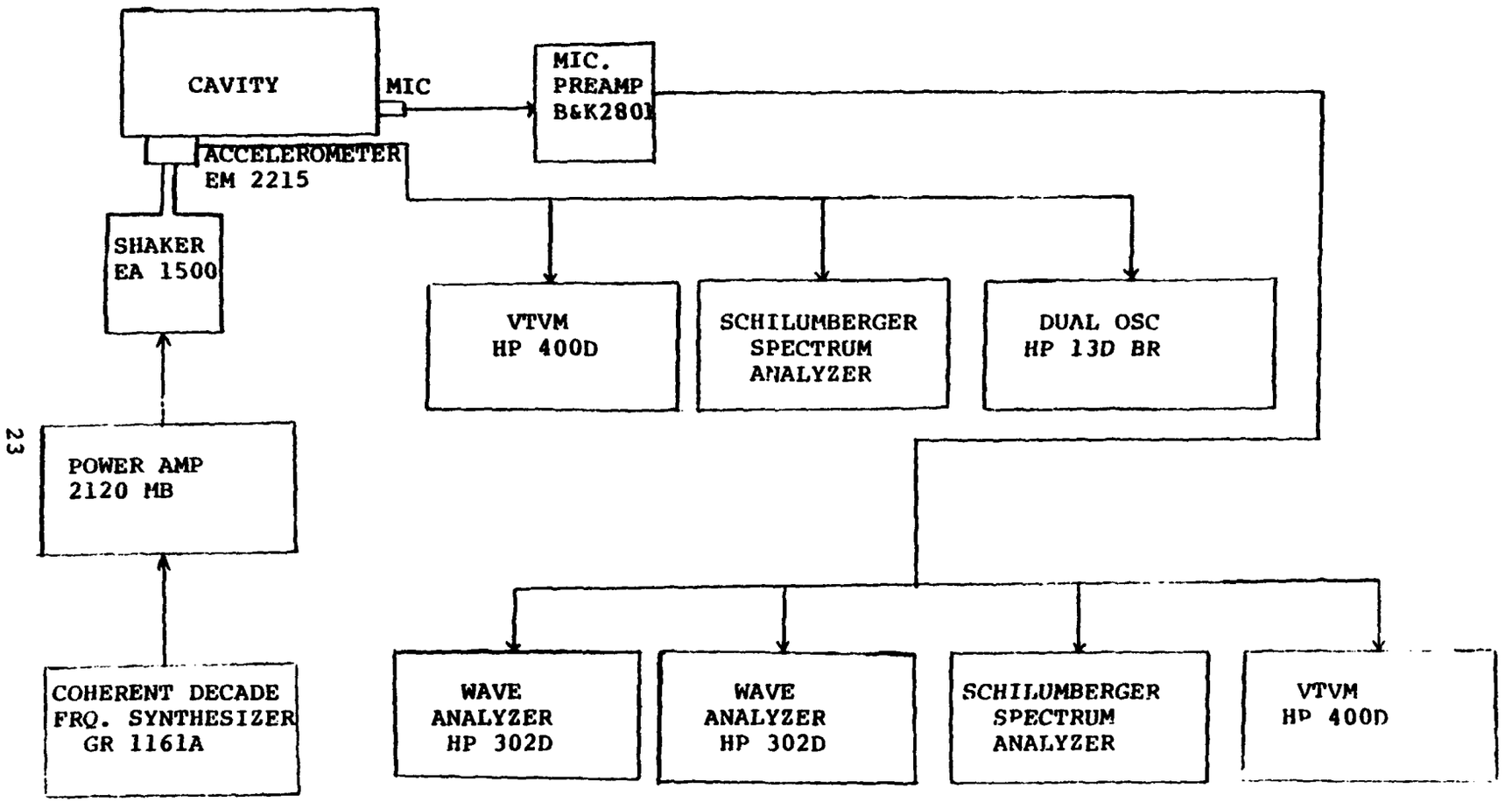

Fig. 4. Block Diagram

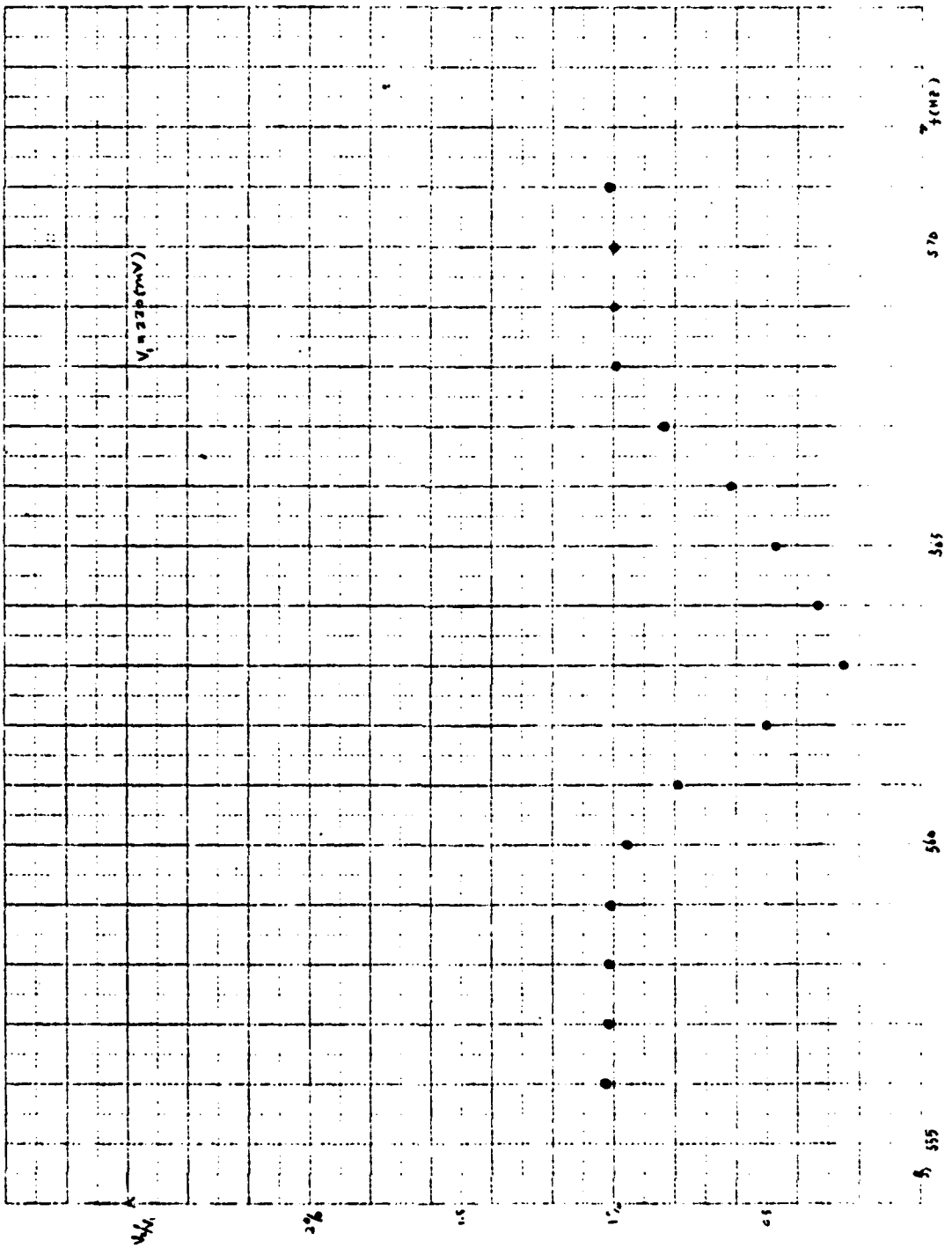

Figure 5

Typical harmonic distortion in output of the accelerometer.

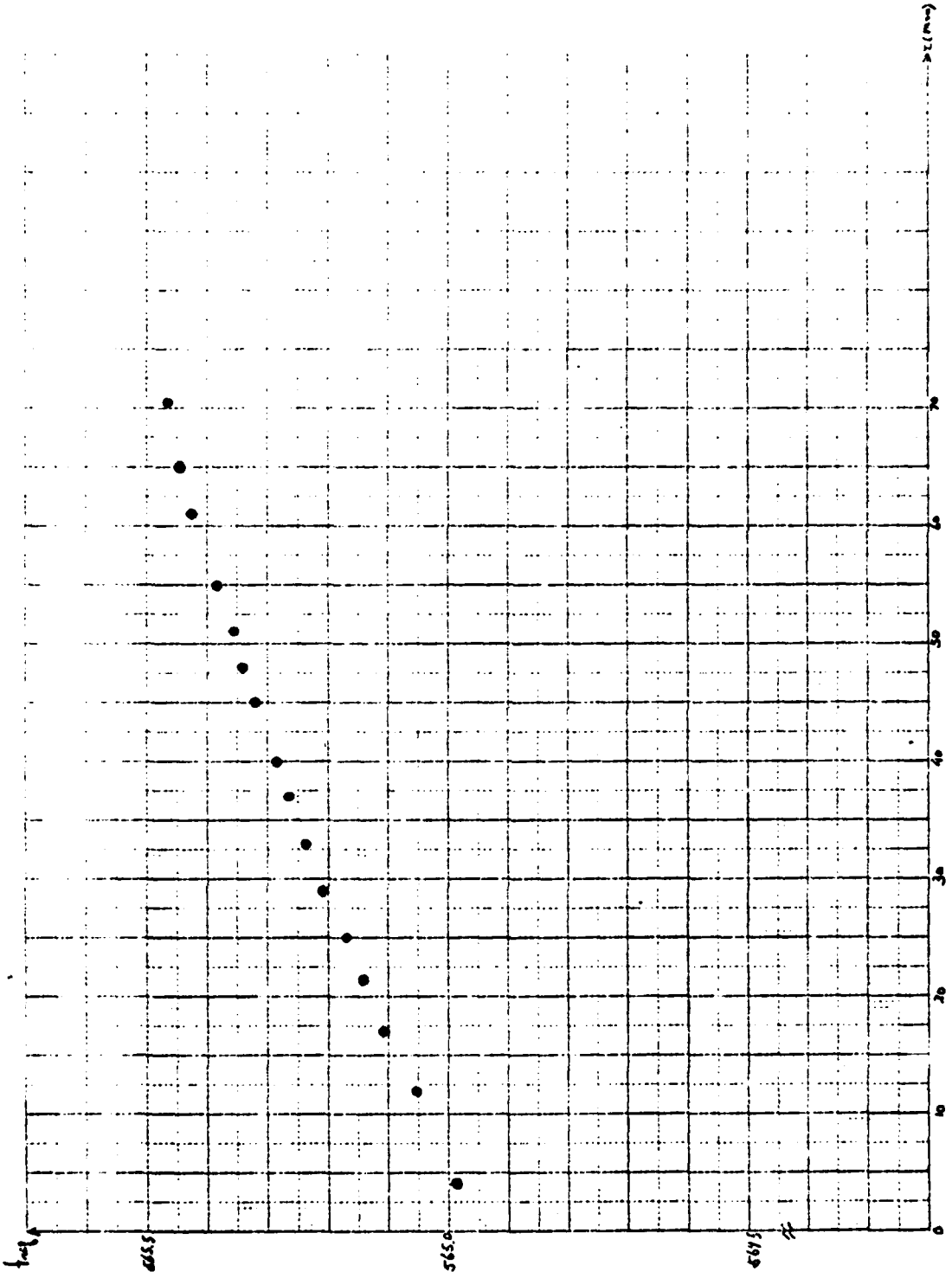

Figure 6

Typical time dependence of the resonance frequency of the lowest standing wave (0,1,0).

APPENDIX A

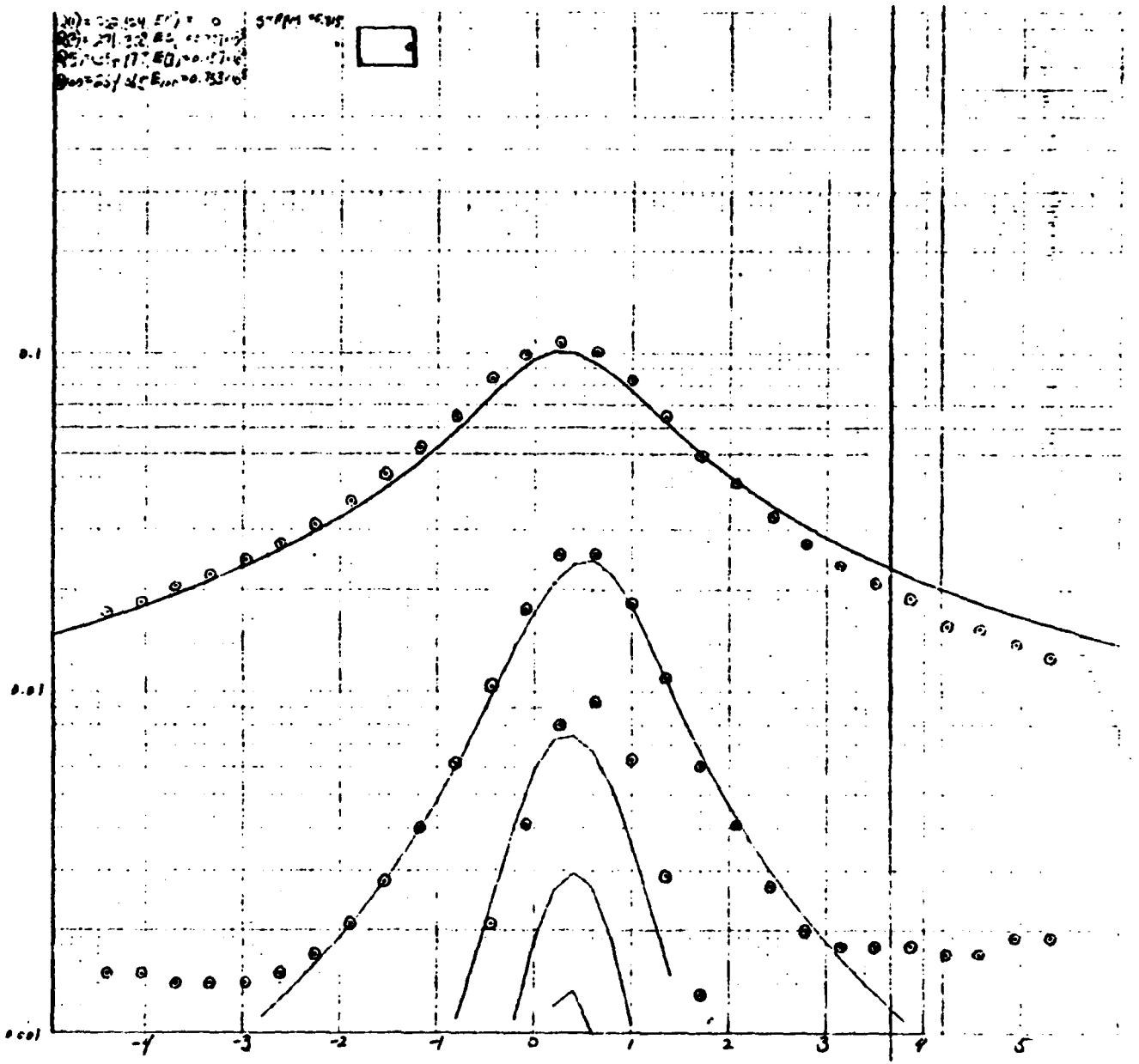

Fig. 7

Fig. 8

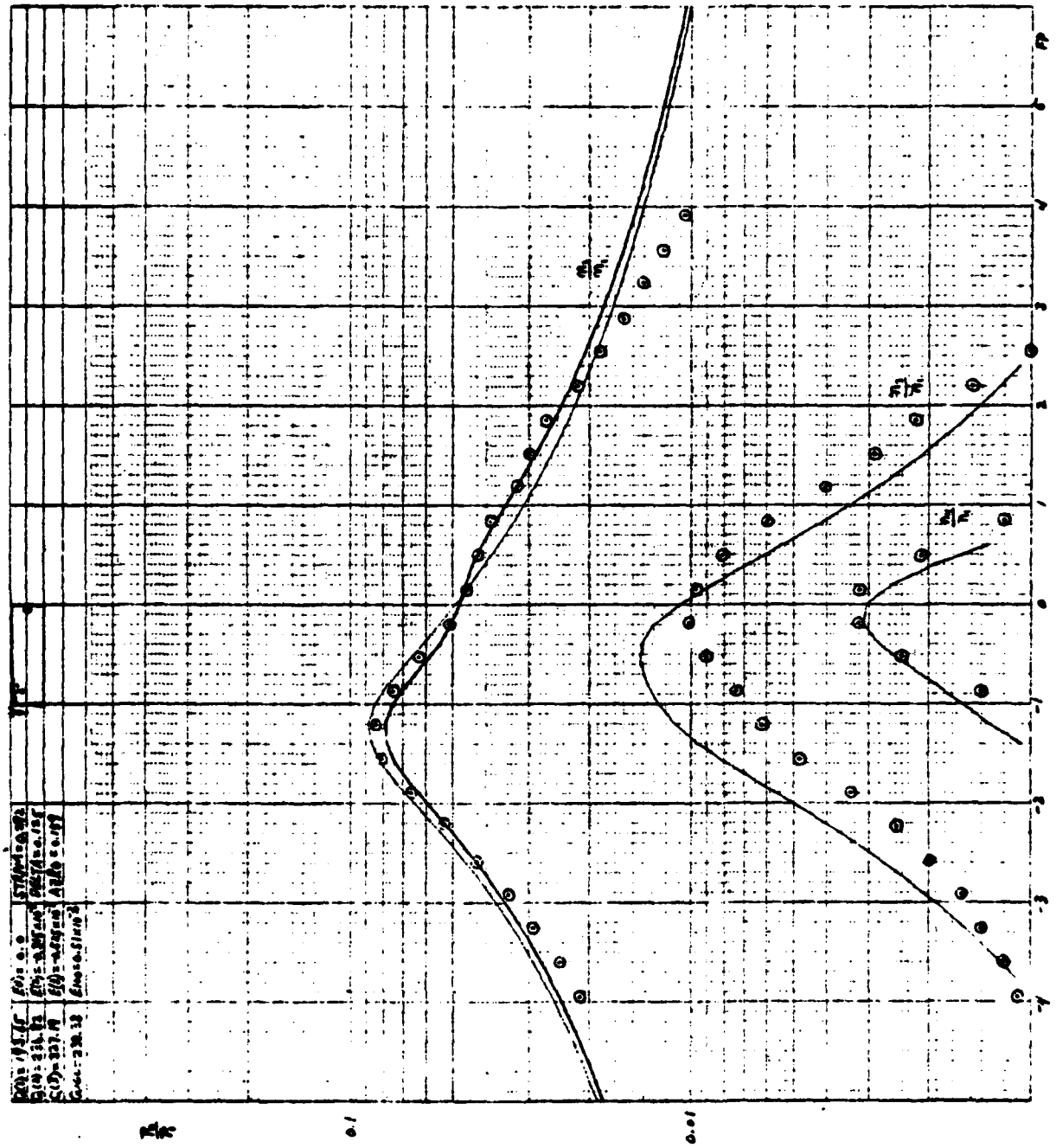

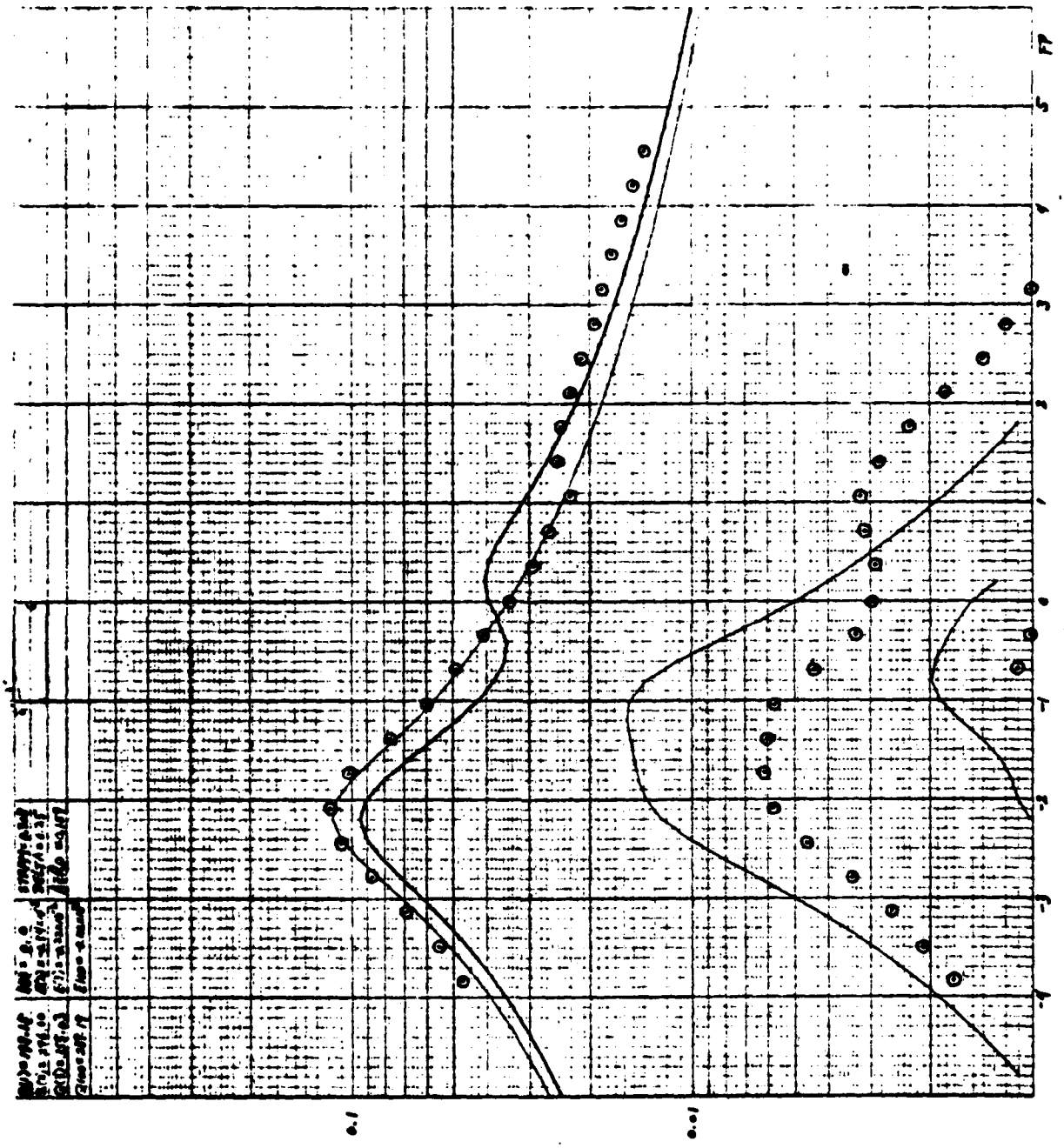

Fig. 6

Fig. 10

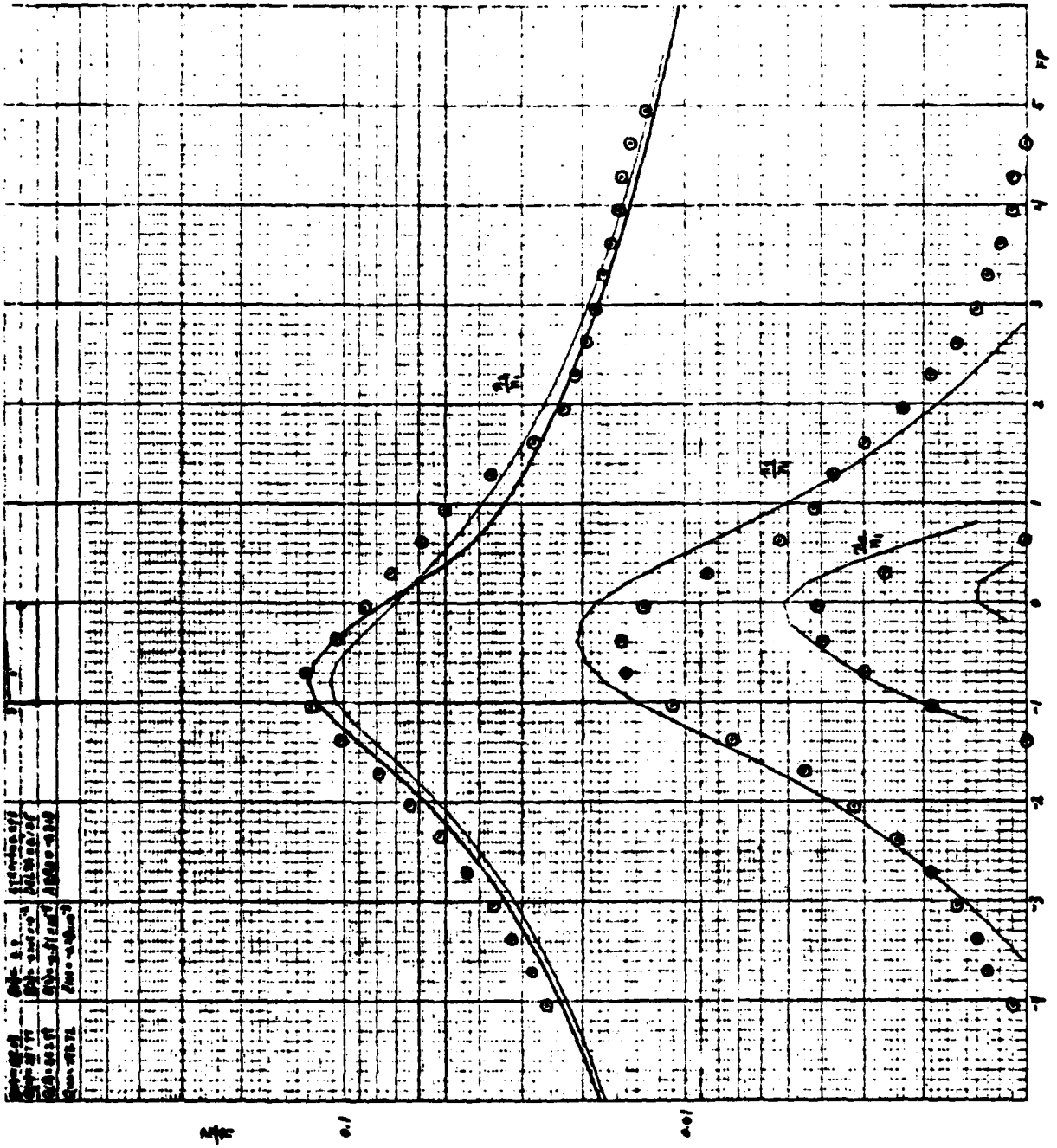

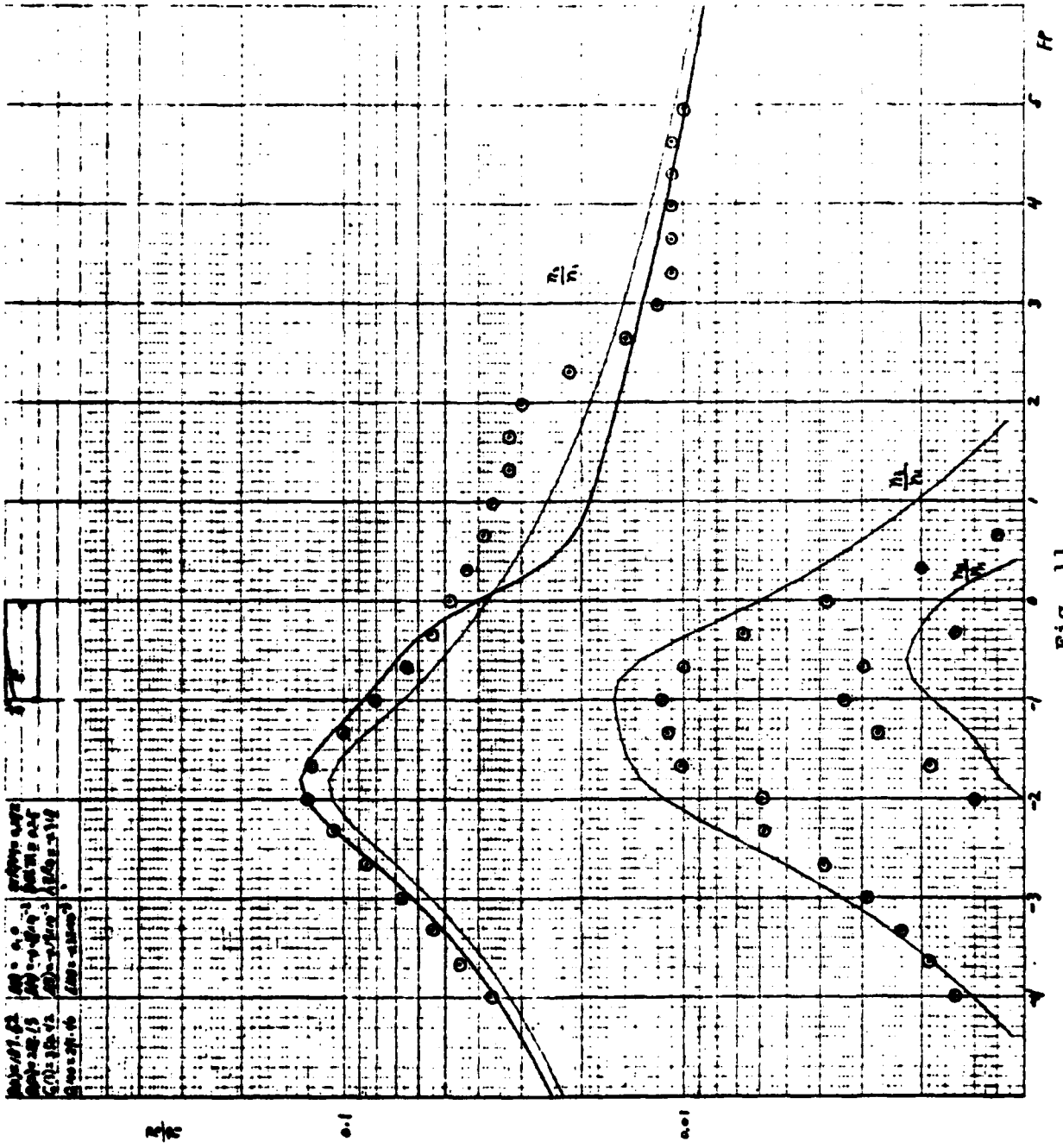

Fig. 11

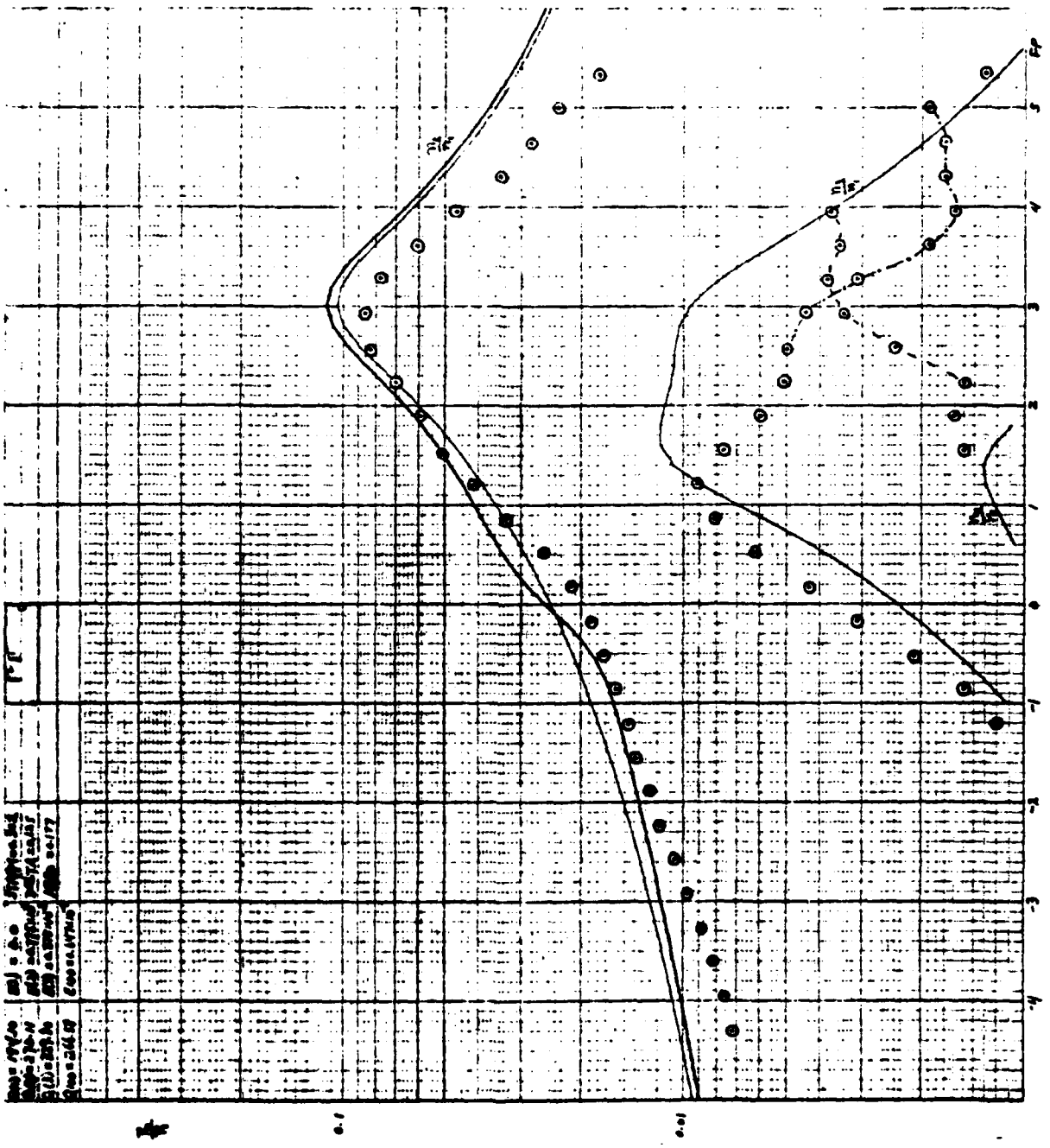

Fig. 12

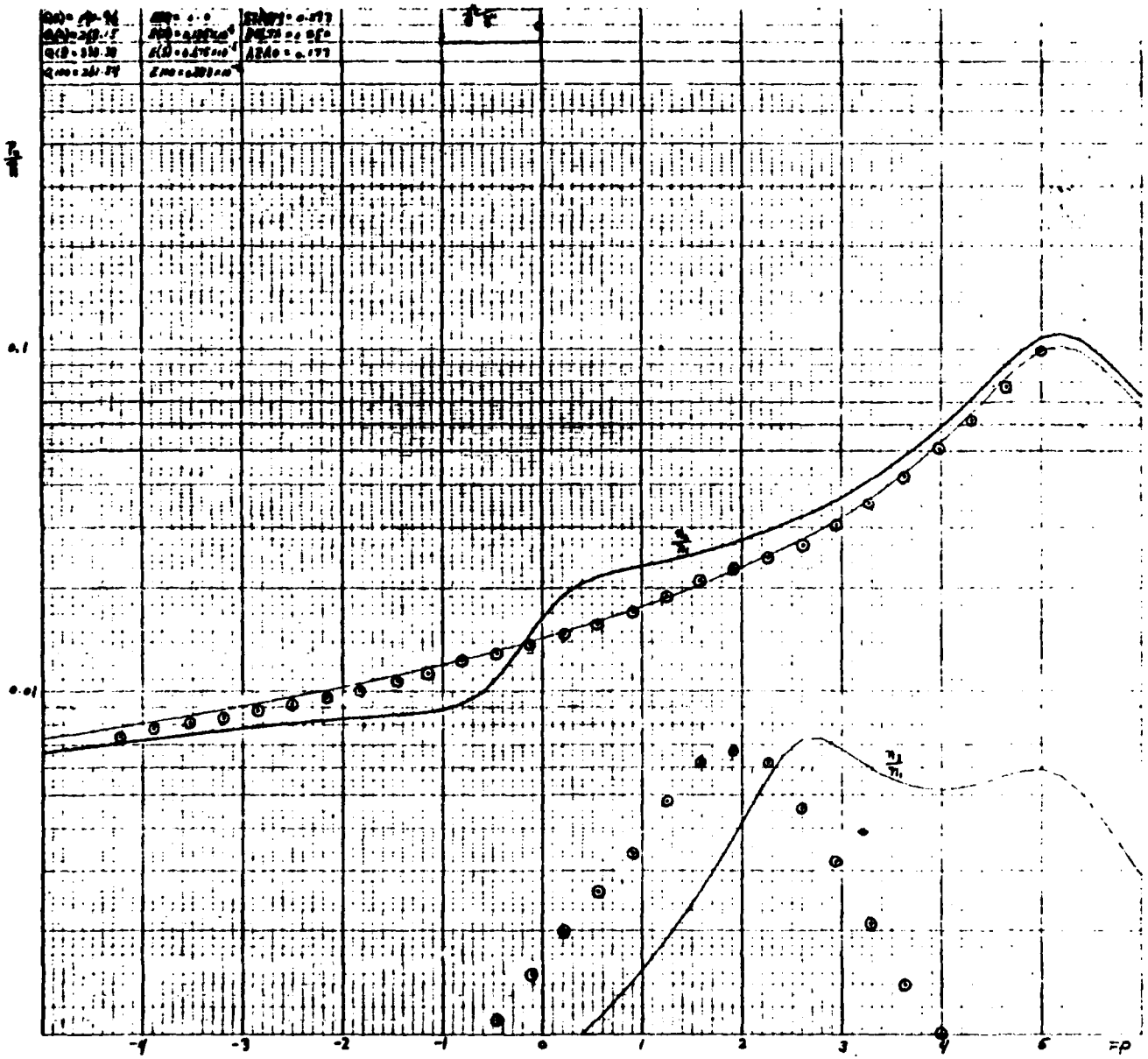

Fig. 13

Fig. 14

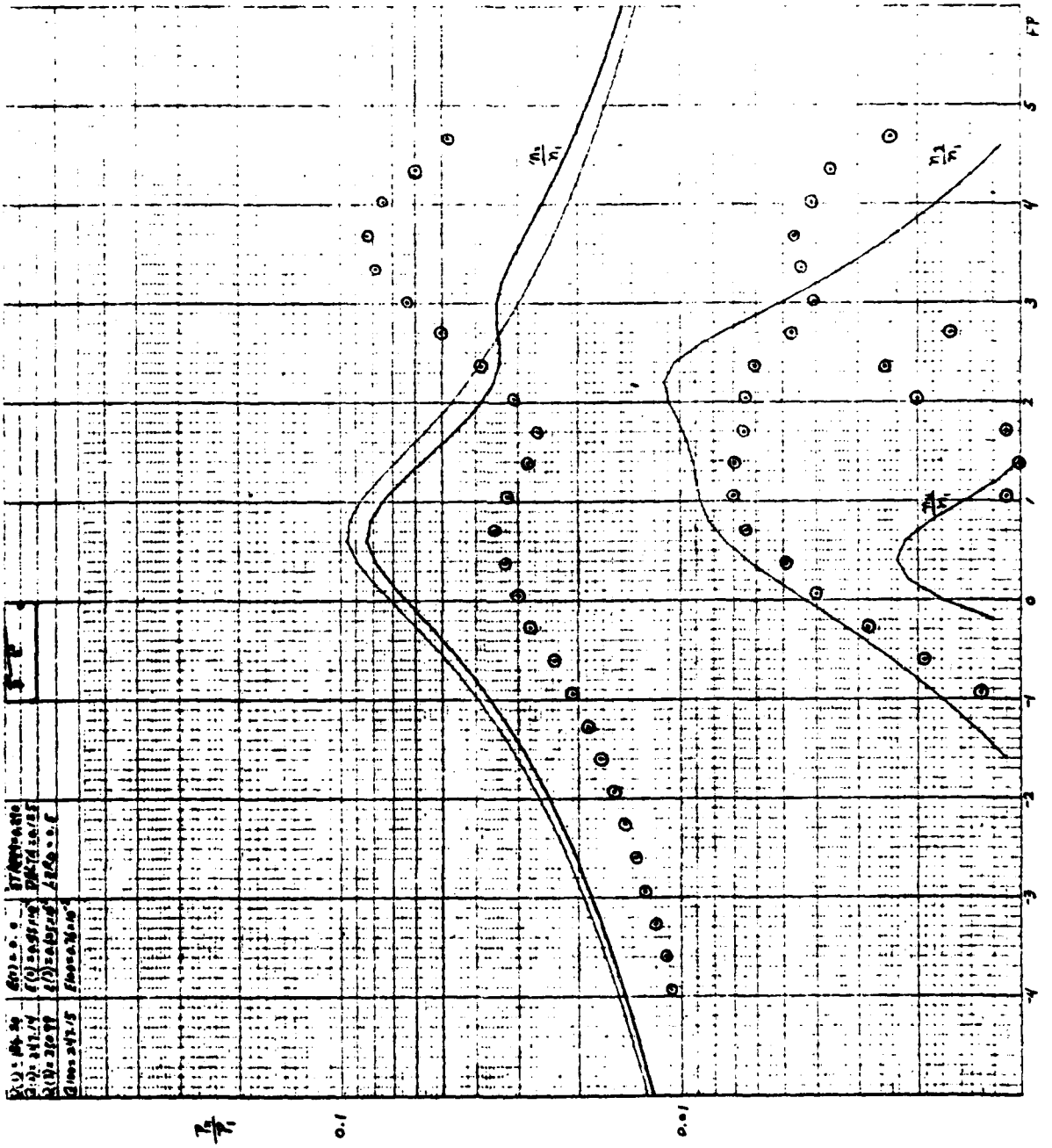

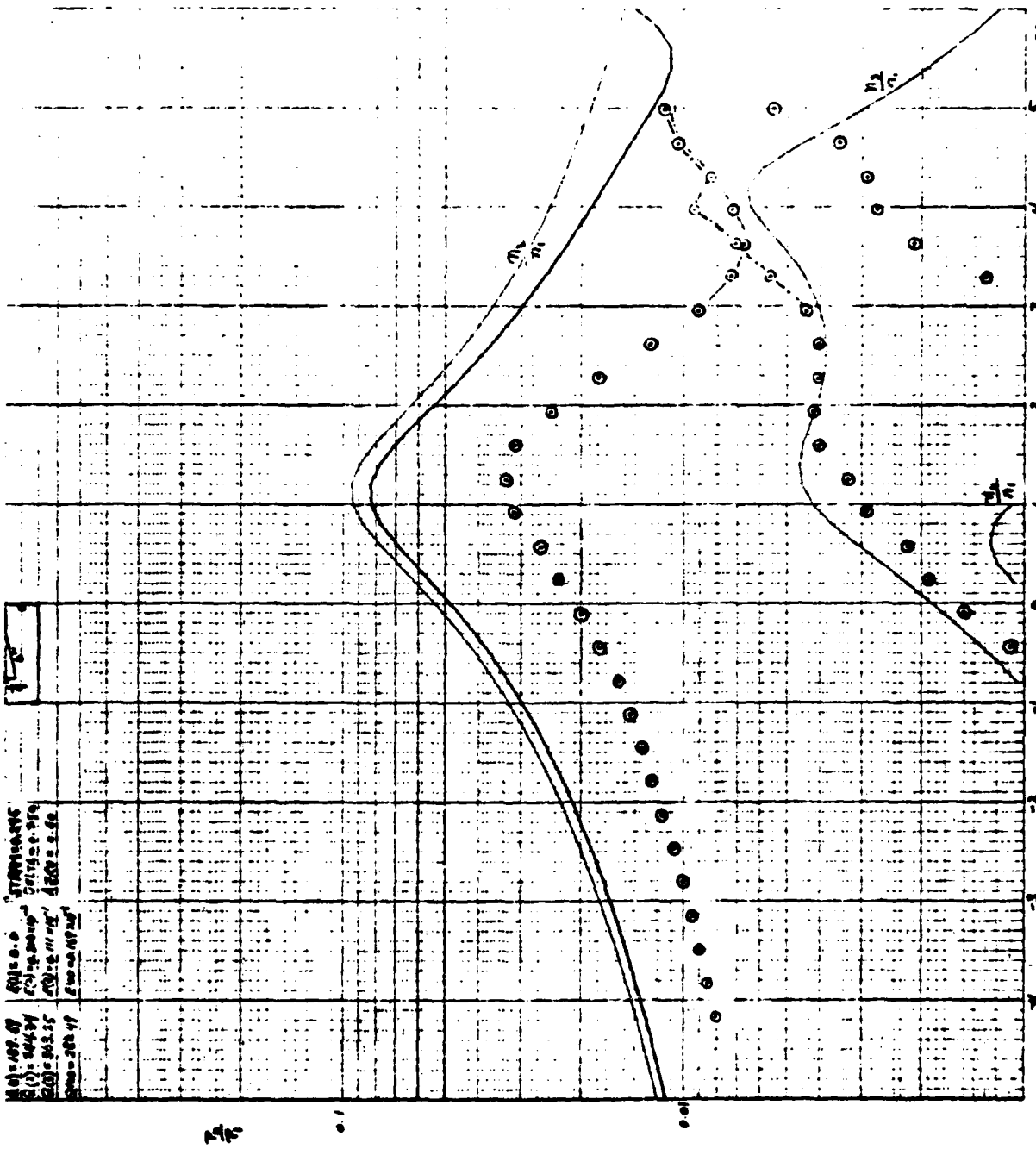

Fig. 15

APPENDIX B

TABLE 0

Mode	Frequency (Hz)	Mode	Frequency (Hz)
010	565	130	2039.4
020	1131	140	2529.0
030	1697	150	3032.0
100	1131	111	2980.5
110	1205	101	2757.5
120	1599.5	011	2926.4

TABLE I (Fig. 7)

mode	time	f_u	f_L	f_r	Q	E
010	0	565.77	562.88	564.33	195.40	0
020	3	1131.84	1127.79	1129.81	278.69	0.10×10^{-2}
030	6	1698.27	1693.52	1695.90	356.51	0.17×10^{-2}
100	9	1131.87	1127.59	1129.73	264.20	-0.74×10^{-4}

V_1 = 11dB time	f	V_2	V_3	V_4	P_2/P_1	P_3/P_1	$P_4/P_.$	FP
12	558.5	-50.0	-70.5	-70.5	0.0113	0.0011	0.0011	-4.19
13	559.0	-47.9	-72.0	-69.0	0.0143	0.0009	0.0013	-3.85
14	559.5	-46.9	-73.8	-67.8	0.0160	———	0.0014	-3.50
15	560.0	-46.0	-72.6	-67.5	0.0179	———	0.0015	-3.15
16	560.5	-44.8	-71.2	-69.7	0.0204	0.0011	0.0012	-2.81
17	561.0	-43.7	-69.7	-73.5	0.0233	0.0012	———	-2.47
18	561.5	-42.4	-67.8	-76.5	0.0269	0.0014	———	-2.12
19	562.0	-41.0	-65.7	-75.9	0.0316	0.0018	———	-1.78
20	562.5	-39.4	-63.2	-82.5	0.0380	0.0025	———	-1.43
21	565.0	-37.8	-60.3	-85.0	0.0457	0.0034	———	-1.09
22	563.5	-35.9	-56.6	-74.9	0.0569	0.0052	———	-0.74
23	564.0	-34.0	-52.2	-67.5	0.0708	0.0007	0.0015	-0.40
24	564.5	-32.2	-47.6	-60.6	0.0876	0.0148	0.0033	-0.05
25	565.0	-31.1	-45.0	-54.5	0.0994	0.0200	0.0067	0.29
26	565.5	-31.6	-43.9	-52.9	0.0933	0.0226	0.0081	0.64
27	566.0	-33.3	-46.7	-56.0	0.0772	0.0164	0.0056	0.98
28	566.5	-35.3	-51.0	-63.2	0.0610	-0.0100	0.0025	1.33
29	567.0	-37.6	-55.5	-70.8	0.0484	0.0060	0.0010	1.67
30	567.5	-39.8	-60.0	-73.6	0.0365	0.0036	———	2.02
31	568.0	-42.1	-64.3	-74.7	0.0279	0.0022	———	2.36
32	568.5	-44.1	-68.5	-74.2	0.0221	0.0013	———	2.71
33	569.0	-46.2	-69.9	———	0.0174	0.0011	———	3.05
34	569.5	-47.2	-68.7	-67.0	0.0156	0.0013	0.0016	3.40
35	570.0	-48.0	-65.4	-67.0	0.0141	0.0019	0.0010	3.14
36	570.5	-48.9	-65.1	-67.2	0.0127	0.0020	0.0016	4.09
37	571.0	-49.8	-65.2	-67.5	0.0115	0.0019	0.0015	4.43
38	571.5	-50.8	-65.4	-68.2	0.0103	0.0019	0.0014	4.78
39	572.0	-51.7	-65.8	-68.6	0.0093	0.0018	0.0013	5.12
40	572.5	-52.5	-66.3	-67.4	0.0084	0.0017	0.0015	3.47
41	573.0	-54.7	-65.1	-66.7	0.0065	0.0020	0.0016	5.81

mode	time	f_u	f_L	f_r	Q	E
010	44	566.28	563.37	564.82	194.03	0
020	47	1132.74	1128.67	1130.71	277.82	0.94×10^{-3}
030	50	1699.77	1694.97	1697.37	353.84	0.17×10^{-2}
100	53	1132.80	1128.48	1130.64	262.03	-0.61×10^{-4}

TABLE II (Fig. 8)

mode	time	f_u	f_L	f_r	Q	E
010	0	568.27	565.28	566.77	189.81	0
020	3	1132.37	1127.62	1129.99	238.25	-0.31×10^{-2}
030	6	1701.89	1696.79	1699.34	333.14	-0.57×10^{-3}
100	9	1132.44	1127.71	1130.07	238.76	0.69×10^{-4}

V_1=-11dB time	f	V_2	V_3	V_4	P_2/P_1	P_3/P_1	P_4/P_1	FP
12	561.3	-44.3	-69.9	-71.3	0.0216	0.0011	———	-3.95
13	561.8	-43.2	-69.2	-72.2	0.0247	0.0012	———	-3.61
14	562.3	-41.7	-68.3	-74.0	0.0293	0.0014	———	-3.26
15	562.8	-40.2	-66.8	-80.0	0.0347	0.0016	———	-2.92
16	563.3	-38.5	-65.2	———	0.0422	0.0020	———	-2.58
17	563.8	-36.4	-62.9	———	0.0537	0.0025	———	-2.24
18	564.3	-34.3	-60.3	———	0.0684	0.0034	———	-1.90
19	564.8	-32.8	-57.2	———	0.0813	0.0049	———	-1.56
20	565.3	-32.5	-55.0	-72.0	0.0841	0.0063	0.0009	-1.22
21	565.8	-33.5	-53.5	-67.8	0.0750	0.0075	0.0014	-0.87
22	566.3	-35.1	-51.8	-62.5	0.0624	0.0092	0.0024	-0.53
23	566.8	-36.9	-50.9	-60.9	0.0507	0.1002	0.0032	-0.19
24	567.3	-37.9	-51.2	-60.8	0.0452	0.0098	0.0032	0.15
25	567.8	-38.6	-52.8	-64.6	0.0419	0.0082	0.0021	0.49
26	568.3	-39.2	-55.3	-69.2	0.0391	0.0061	0.0072	0.83
27	568.8	-40.3	-58.7	-75.0	0.0343	0.0041	———	1.78
28	569.3	-41.5	-61.7	-78.5	0.0300	0.0029	———	1.52
29	569.8	-42.4	-64.3	———	0.0271	0.0022	———	1.86
30	570.3	-44.3	-67.3	———	0.0218	0.0015	———	2.20
31	570.8	-45.5	-70.8	———	0.0188	0.0010	———	2.54
32	571.3	-46.9	-75.0	———	0.0160	0.0006	———	2.88
33	571.8	-48.1	-76.9	———	0.0140	0.0005	———	3.22
34	572.3	-49.3	-75.2	-69.1	0.0122	0.0006	0.0012	3.57
35	572.8	-50.6	-73.5	-68.0	0.0105	0.0007	0.0014	3.91
36	573.3	-51.0	-71.7	-66.5	0.0100	0.0009	0.0017	4.25
37	573.8	-51.8	-71.1	-66.0	0.0092	0.0010	0.0018	4.59
38	574.3	-52.5	-70.3	-65.7	0.0084	0.0011	0.0019	4.93
39	574.8	053.8	-72.3	-66.7	0.0073	0.009	0.0016	5.27

mode	time	f_u	f_2	f_r	Q	E
010	42	568.82	565.95	567.38	197.49	0
020	45	1133.50	1128.70	1131.10	235.40	-0.32×10^{-2}
030	48	1703.98	1698.69	1701.34	321.25	-0.48×10^{-3}
100	51	1133.85	1129.10	1131.47	238.00	0.33×10^{-3}

TABLE III (Fig. 9)

mode	time	f_u	f_2	f_r	Q	E
010	0	567.85	565.01	566.43	199.52	0
020	3	1128.61	1124.81	1126.71	296.58	-0.54×10^{-2}
030	6	1697.95	1693.16	1695.39	354.31	-0.23×10^{-2}
100	9	1128.77	1124.87	1126.82	288.63	-0.96×10^{-4}

V_1=-11dB	time	f	V_2	V_3	V_4	P_2/P_1	P_3/P_1	P_4/P_1	FP
	12	561.0	-37.6	-66.2	———	0.0468	0.0017	———	-3.84
	13	561.5	-36.2	-64.8	———	0.0550	0.0021	———	-3.49
	14	562.0	-34.3	-62.8	———	0.0684	0.0026	———	-3.14
	15	562.5	-32.2	-60.3	———	0.0876	0.0034	———	-2.79
	16	563.0	-30.2	-57.5	-76.0	0.1096	0.0047	0.0006	-2.44
	17	563.5	-29.5	-55.6	-73.4	0.1189	0.0059	0.0008	-2.09
	18	564.0	-30.8	-55.2	-74.0	0.1023	0.0062	0.0007	-1.74
	19	564.5	-33.3	-55.5	-74.7	0.0772	0.0060	0.0007	-1.39
	20	565.0	-35.5	-55.8	-71.8	0.0599	0.0058	0.0009	-1.04
	21	565.5	-37.3	-58.0	-70.2	0.0484	0.0045	0.0011	-0.67
	22	566.0	-38.9	-60.5	-71.4	0.0403	0.0033	0.0010	-0.34
	23	566.5	-40.3	-61.5	-76.0	0.0345	0.0030	0.0006	0.00
	24	567.0	-41.7	-61.7	-80.0	0.0293	0.0029	———	0.36
	25	567.5	-42.5	-61.3	-81.3	0.0266	0.0031	———	0.71
	26	568.0	-42.6	-60.8	-80.3	0.0263	0.0032	———	1.06
	27	568.5	-43.1	-62.2	———	0.0250	0.0028	———	1.41
	28	569.0	-43.3	-63.7	———	0.0243	0.0023	———	1.76
	29	569.5	-43.8	-65.9	———	0.0230	0.0018	———	2.11
	30	570.0	-44.5	-68.0	———	0.0213	0.0014	———	2.46
	31	570.5	-45.2	-69.6	———	0.0196	0.0012	———	2.81
	32	571.0	-45.6	-70.9	———	0.0186	0.0010	———	3.16
	33	571.5	-46.2	-71.7	———	0.0174	0.0009	———	3.51
	34	572.0	-46.8	-72.7	———	0.0162	———	———	3.86
	35	572.5	-47.5	-73.3	———	0.0150	———	———	4.21
	36	573.0	-47.5	-73.5	———	0.0150	———	———	4.56
	37	573.5	-48.2	-77.0	———	0.0139	———	———	4.91

mode	time	f_u	f_L	f_r	Q	E
010	40	567.99	565.11	566.55	196.79	0
020	43	1128.94	1125.12	1127.03	295.42	-0.54×10^{-2}
030	46	1698.43	1693.67	1696.05	355.76	-0.21×10^{-2}
100	49	1129.10	1125.21	1127.15	289.76	0.11×10^{-3}

TABLE IV (Fig. 10)

mode	time	f_u	f_L	f_r	Q	E
010	0	566.19	563.20	564.70	189.30	0
020	3	1128.86	1124.95	1126.91	287.70	-0.2×10^{-2}
030	6	1696.18	1691.38	1693.78	353.24	-0.18×10^{-3}
100	9	1128.46	1124.62	1126.54	293.29	-0.32×10^{-3}

V_1=-11dB	time	f	V_2	V_3	V_4	P_2/P_1	P_3/P_1	P_4/P_1	FP
	12	558.7	-42.8	-69.8	———	0.0257	0.0011	———	-4.04
	13	559.2	-41.8	-68.7	———	0.0288	0.0013	———	-3.71
	14	559.7	-40.8	-67.9	———	0.0324	0.0014	———	-3.37
	15	560.2	-39.7	-66.9	———	0.0367	0.0016	———	-3.04
	16	560.7	-38.3	-65.5	———	0.0434	0.0019	———	-2.71
	17	561.2	-36.7	-63.5	———	0.0519	0.0024	———	-2.38
	18	561.7	-34.9	-61.0	———	0.0638	0.0032	———	-2.04
	19	562.2	-33.0	-57.8	-76.3	0.9794	0.0046	———	-1.71
	20	562.7	-30.7	-53.7	-70.7	0.1041	0.0074	0.0010	-1.38
	21	563.2	-28.9	-50.2	-65.3	0.1274	0.0110	0.0019	-1.04
	22	563.7	-28.5	-47.5	-61.4	0.1334	0.0150	0.0030	-0.71
	23	564.2	-30.4	047.2	-59.0	0.1078	0.0155	0.0040	-0.38
	24	564.7	-32.2	-48.5	-58.5	0.0873	0.0133	0.0042	-0.05
	25	565.2	-33.7	-52.2	-62.7	0.0733	0.0087	0.0026	0.29
	26	565.7	-35.6	-56.4	-70.07	0.0592	0.0054	0.0010	0.62
	27	566.2	-37.0	-58.4	-74.7	0.0501	0.0043	———	0.95
	28	566.7	-39.6	-59.7	-77.2	0.0314	0.0037	———	1.29
	29	567.2	-42.1	-61.5	———	0.0279	0.0030	———	1.62
	30	567.7	-43.7	-63.7	———	0.0232	0.0023	———	1.95
	31	568.2	-44.5	-65.5	———	0.0221	0.0019	———	2.29
	32	568.7	-45.1	-66.9	———	0.0197	0.0016	———	2.62
	33	569.2	-45.6	-68.0	———	0.0186	0.0014	———	2.95
	34	569.7	-46.1	-69.0	———	0.0176	0.0013	———	3.29
	35	570.2	-46.6	-69.8	———	0.0167	0.0012	———	3.62
	36	570.7	-47.0	-70.4	———	0.0158	0.0011	———	3.95
	37	571.2	-47.2	-70.6	———	0.0155	0.0011	———	4.28
	38	571.7	-47.7	-71.3	———	0.0146	0.0010	———	4.62
	39	572.2	-48.6	-63.9	———	0.0132	0.0023	———	4.95

mode	time	f_u	f_L	f_r	Q	E
010	42	566.35	563.33	564.84	186.79	0
020	45	1129.43	1125.53	1127.48	1287.84	-0.19×10^{-2}
030	48	1697.04	1692.26	1694.65	353.94	-0.78×10^{-4}
100	51	1129.12	1125.28	1127.20	294.16	-0.24×10^{-3}

TABLE V (Fig. 11)

mode	time	f_u	f_L	f_r	Q	E
010	0	566.90	563.86	565.38	185.80	0
020	3	1127.19	1123.28	1125.23	288.08	-0.49×10^{-2}
030	6	1695.31	1690.47	1692.89	349.27	-0.19×10^{-2}
100	9	1126.76	1122.90	1124.83	291.41	-0.36×10^{-3}

V_1=-11dB time	f	V_2	V_3	V_4	P_2/P_1	P_3/P_1	P_4/P_1	FP
12	559.4	-39.5	-66.9	———	0.0376	0.0016	———	-3.99
13	559.9	-37.9	-65.3	———	0.045	0.0019	———	-3.66
14	560.4	-36.4	-63.9	———	0.054	0.0023	———	-3.33
15	560.9	-34.5	-61.8	———	0.0672	0.0029	———	-3.00
16	561.4	-32.4	-59.1	-78.0	0.0856	0.0039	———	-2.66
17	561.9	-30.3	-55.7	-72.7	0.109	0.0058	0.0008	-2.33
18	562.4	-28.7	-55.6	-68.2	0.131	0.0059	0.0014	-2.00
19	562.9	-28.9	-50.8	-65.3	0.127	0.0103	0.0017	-1.67
20	563.4	-30.9	-50.0	-62.5	0.101	0.0112	0.0027	-1.34
21	563.9	-32.3	-49.7	-60.3	0.081	0.0116	0.0034	-1.01
22	564.4	-34.7	-50.9	-61.4	0.065	0.0101	0.0030	-0.67
23	564.9	-36.3	-54.3	-67.0	0.055	0.0068	0.0016	-0.34
24	565.4	-37.5	-59.3	-75.2	0.048	0.0038	———	-0.01
25	565.9	-38.4	-65.0	———	0.043	0.0020	———	-0.32
26	566.4	-39.3	-69.7	———	0.039	0.0012	———	-0.65
27	566.9	-39.7	-72.2	———	0.037	0.0009	———	0.98
28	567.4	-40.6	-74.5	———	0.033	———	———	1.32
29	567.9	-40.7	-75.4	———	0.030	———	———	1.65
30	568.4	-41.6	-73.5	———	0.030	———	———	1.98
31	568.9	-44.0	-71.5	———	0.022	0.0009	———	2.31
32	569.4	-47.3	-70.9	———	0.015	0.0010	———	2.64
33	569.9	-49.1	-71.1	———	0.012	0.0010	———	2.97
34	570.4	-49.9	-71.6	———	0.011	———	———	3.31
35	570.9	-50.0	-71.8	———	0.011	———	———	3.64
36	571.4	-50.3	-72.3	———	0.011	———	———	3.97
37	571.9	-50.4	-72.4	———	0.011	———	———	4.30
38	572.4	-50.4	-72.4	———	0.011	———	———	4.63
39	572.9	-51.1	-71.6	———	0.010	———	———	4.96

mode	time	f_u	f_L	f_r	Q	E
010	42	566.95	563.96	565.46	189.24	0
020	45	1127.31	1123.40	1125.37	288.18	-0.49×10^{-2}
030	48	1695.54	1690.73	1093.14	351.57	-0.27×10^{-3}
100	51	1126.98	1123.12	1125.05	291.39	-0.27×10^{-3}

TABLE VI (Fig. 12)

mode	time	f_u	f_L	f_r	Q	E
010	0	564.94	562.04	563.49	194.44	0
020	3	1137.75	1133.55	1135.65	270.78	0.77×10^{-2}
030	6	1699.31	1694.34	1696.82	341.28	0.28×10^{-2}
100	9	1137.85	1133.56	1135.71	264.96	0.48×10^{-4}

V_1=-11dB	time	f	V_2	V_3	V_4	P_2/P_1	P_3/P_1	P_4/P_1	FP
	12	557.5	-53.7	-73.9	-76.2	0.0073	0.0007	———	-4.30
	13	558.0	-53.3	-74.2	-76.3	0.0077	———	———	-3.96
	14	558.5	-52.6	-74.6	-77.3	0.0083	———	———	-3.62
	15	559.0	-52.0	-75.1	-80.2	0.0089	———	———	-3.27
	16	559.5	-51.2	-85.3	-85.0	0.0098	———	———	-2.93
	17	560.0	-50.4	-75.3	———	0.0107	———	———	-2.58
	18	560.5	-49.6	-74.9	———	0.0117	———	———	-2.24
	19	561.0	-49.0	-73.3	———	0.0126	0.0008	———	-1.89
	20	561.5	-48.2	-71.6	———	0.0139	0.0009	———	-1.55
	21	562.0	-47.7	-69.7	———	0.0146	0.0012	———	-1.21
	22	562.5	-47.1	-67.2	———	0.0158	0.0015	———	-0.86
	23	563.0	-46.3	-64.7	———	0.0172	0.0021	———	-0.52
	24	563.5	-45.5	-61.3	———	0.0188	0.0031	———	-0.17
	25	564.0	-44.4	-58.1	———	0.0215	0.0044	———	0.17
	26	564.5	-42.7	-55.0	———	0.0260	0.0063	———	0.52
	27	565.0	-40.5	-52.7	———	0.0335	0.0082	———	0.86
	28	565.5	-38.8	-51.8	-56.5	0.0407	0.0092	———	1.21
	29	566.0	-37.0	-53.3	-67.5	0.0504	0.0077	0.0015	1.55
	30	566.5	-35.5	-55.5	-67.0	0.0596	0.0060	0.0016	1.89
	31	567.0	-34.1	-56.6	-67.5	0.0700	0.0052	0.0015	2.24
	32	567.5	-32.8	-56.9	-63.3	0.0813	0.0051	0.0024	2.58
	33	568.0	-32.3	-57.9	-60.3	0.0861	0.0045	0.0034	2.93
	34	568.5	-33.3	-61.3	-59.3	0.0072	0.0031	0.0038	3.27
	35	569.0	-35.4	-65.5	-60.0	0.0603	0.0019	0.0035	3.61
	36	569.5	-37.8	-67.0	-59.7	0.0457	0.0016	0.0037	3.96
	37	570.0	-40.2	-66.6	-60.0	0.0349	0.0017	0.0035	4.30
	38	570.5	-42.0	-66.2	-60.3	0.0282	0.0017	0.0034	4.65
	39	571.0	-43.6	-65.6	-60.5	0.0236	0.0019	0.0033	4.99
	40	571.5	-46.0	-68.6	-62.0	0.0178	0.0013	0.0028	5.34

mode	time	f_u	f_L	f_r	Q	E
010	43	565.47	562.56	564.01	193.75	0
020	46	1138.89	1134.67	1136.78	269.44	0.78×10^{-2}
030	49	1700.94	1695.60	1698.27	318.33	0.37×10^{-2}
100	52	1139.00	1134.76	1136.88	268.20	0.81×10^{-4}

TABLE VII (Fig. 13)

mode	time	f_u	f_L	f_r	Q	E
010	0	561.56	558.62	560.09	190.57	0
020	3	1137.45	1133.15	1135.30	264.33	0.14×10^{-1}
030	6	1694.09	1689.09	1691.59	338.39	0.67×10^{-2}
100	9	1137.58	1133.26	1135.42	263.01	0.11×10^{-3}

V_1=-11dB	time	f	V_2	V_3	V_4	P_2/P_1	P_3/P_1	P_4/P_1	FP
	12	554.1	-53.6	-74.7	———	0.0074	0.0007	———	-4.21
	13	554.6	-53.0	-74.7	———	0.0079	0.0007	———	-3.87
	14	555.1	-52.7	-74.7	———	0.0082	0.0007	———	-3.53
	15	555.6	-52.4	-75.5	———	0.0085	0.0006	———	-3.19
	16	556.1	-52.0	-76.1	———	0.0089	0.0006	———	-2.85
	17	556.6	-51.6	-76.7	———	0.0093	0.0005	———	-2.51
	18	557.1	-51.3	-77.5	———	0.0097	0.0005	———	-2.17
	19	557.6	-50.9	-77.5	———	0.0101	0.0005	———	-1.83
	20	558.1	-50.3	-76.9	———	0.0108	0.0005	———	-1.48
	21	558.6	-49.9	-75.1	———	0.0114	0.0006	———	-1.14
	22	559.1	-49.2	-72.8	———	0.0124	0.0008	———	-0.80
	23	559.6	-48.7	-70.3	———	0.0130	0.0011	———	-0.46
	24	560.1	-48.2	-67.5	———	0.0139	0.0015	———	-0.12
	25	560.6	-47.6	-65.0	———	0.0148	0.0020	———	0.22
	26	561.1	-47.0	-62.7	———	0.0158	0.0026	———	0.56
	27	561.6	-46.3	-60.4	———	0.0172	0.0034	———	0.90
	28	561.1	-45.4	-57.2	———	0.191	0.0049	———	1.24
	29	562.6	-44.5	-55.0	———	0.0211	0.0063	———	1.58
	30	563.1	-43.8	-54.4	———	0.0230	0.0068	———	1.92
	31	563.6	-43.1	-55.0	———	0.0248	0.0063	———	2.26
	32	564.1	-42.4	-57.5	———	0.0269	0.0047	———	2.61
	33	564.6	-41.2	-60.9	———	0.0309	0.0032	———	2.95
	34	565.1	-40.0	-64.5	———	0.0355	0.0021	———	3.29
	35	565.6	-38.6	-67.9	———	0.0417	0.0014	———	3.63
	36	566.1	-37.0	-70.6	———	0.0501	0.0010	———	3.97
	37	566.6	-35.2	-73.7	———	0.0617	0.0070	———	4.31
	38	567.1	-33.2	-71.0	———	0.0776	0.0010	———	4.65
	39	567.6	-31.5	-66.3	———	0.0944	0.0017	———	4.99

mode	time	f_u	f_L	f_r	Q	E
010	43	561.94	559.01	560.47	191.35	0
020	46	1138.34	1134.01	1136.18	261.97	0.14×10^{-1}
030	49	1695.35	1690.34	1692.85	338.37	0.68×10^{-2}
100	52	1138.44	1134.07	1136.25	260.07	0.69×10^{-4}

TABLE VIII (Fig. 14)

mode	time	f_u	f_L	f_r	Q	E
010	0	564.94	561.90	563.42	185.40	0
020	3	1137.18	1126.60	1128.89	246.64	0.18×10^{-2}
030	6	1703.17	1698.34	1700.75	352.63	0.62×10^{-2}
100	9	1139.73	1135.13	1137.43	247.16	0.76×10^{-2}

V_1=-11dB	time	f	V_2	V_3	V_4	P_2/P_1	P_3/P_1	P_4/P_1	FP
	12	557.5	-50.4	-74.2	———	0.0107	———	———	-3.92
	13	558.0	-50.0	-74.2	———	0.0112	———	———	-3.59
	14	558.5	-49.5	-74.2	———	0.0120	———	———	-3.26
	15	559.0	-48.9	-74.3	———	0.0127	———	———	-2.93
	16	559.5	-48.4	-74.5	———	0.0136	———	———	-2.59
	17	560.0	-47.7	-74.3	———	0.0147	———	———	-2.26
	18	560.5	-47.0	-73.9	———	0.0158	———	———	-1.93
	19	561.0	-46.3	-73.0	———	0.0172	———	———	-1.60
	20	561.5	-45.5	-71.1	———	0.0188	0.0010	———	-1.27
	21	562.0	-44.6	-68.5	———	0.0209	0.0013	———	-0.94
	22	562.5	-43.6	-65.3	———	0.0236	0.0019	———	-0.61
	23	563.0	-42.5	-62.1	———	0.0267	0.0028	———	-0.28
	24	563.5	-41.5	-59.3	———	0.0299	0.0039	———	0.05
	25	564.0	-40.6	-57.0	-76.0	0.0331	0.0050	———	0.38
	26	564.5	-40.0	-54.7	-71.8	0.0355	0.0065	0.0009	0.71
	27	565.0	-40.8	-54.0	-70.5	0.0324	0.0071	0.0011	1.04
	28	565.5	-42.0	-54.1	-71.3	0.0282	0.0070	0.0010	1.37
	29	566.0	-42.6	-54.7	-70.2	0.0265	0.0066	0.0011	1.70
	30	566.5	-41.2	-54.7	-64.8	0.0310	0.0065	0.0020	2.03
	31	567.0	-39.3	-55.3	-63.0	0.0387	0.0061	0.0025	2.36
	32	567.5	-37.0	-57.4	-67.2	0.0501	0.0048	0.0010	2.69
	33	568.0	-35.0	-58.7	-72.3	0.0631	0.0041	0.0009	3.02
	34	568.5	-33.0	-58.0	-75.5	0.0794	0.0045	———	3.35
	35	569.0	-32.6	-57.5	-79.0	0.0832	0.0047	———	3.68
	36	569.5	-33.6	-58.5	———	0.0741	0.0042	———	4.02
	37	570.0	-35.5	059.9	———	0.0596	0.0036	———	4.35
	38	570.5	-37.4	-63.5	———	0.0480	0.0024	———	4.68

mode	time	f_u	f_L	f_r	Q	E
010	0	564.94	561.93	563.43	187.00	0
020	3	1131.26	1126.70	1128.98	247.64	0.19×10^{-2}
030	6	1703.35	1698.48	1700.92	349.34	0.63×10^{-2}
100	9	1139.88	1135.27	1137.58	247.14	0.76×10^{-2}

TABLE VIII (Fig. 15)

mode	time	f_u	f_L	f_r	Q	E
010	0	561.20	558.27	559.73	190.78	0
020	3	1125.25	1120.66	1122.96	244.76	0.31×10^{-2}
030	6	1700.26	1695.60	1697.93	364.21	0.11×10^{-1}
100	9	1143.88	1139.80	1141.84	280.07	0.17×10^{-1}

V_1=-11dB	time	f	V_2	V_3	V_4	P_2/P_1	P_3/P_1	P_4/P_1	FP
	12	553.7	-52.7	-77.8	———	0.0082	0.0005	———	-4.17
	13	554.2	-52.4	-78.2	———	0.0086	———	———	-3.83
	14	554.7	-51.8	-78.2	———	0.0091	———	———	-3.49
	15	555.2	-51.4	-78.4	———	0.0095	———	———	-3.15
	16	555.7	-51.0	-79.0	———	0.0100	———	———	-2.81
	17	556.2	-50.5	-79.5	———	0.0107	———	———	-2.47
	18	556.7	-49.7	-79.5	———	0.0116	———	———	-2.13
	19	557.2	-49.1	-78.9	———	0.0124	———	———	-1.79
	20	558.2	-47.8	-75.7	———	0.0145	———	———	-1.12
	21	558.7	-47.0	-72.7	———	0.0158	———	———	-0.78
	22	559.2	-46.0	-70.0	———	0.0178	0.0011	———	-0.44
	23	559.7	-45.0	-67.3	———	0.0200	0.0015	———	-0.10
	24	560.2	-43.6	-65.3	———	0.0234	0.0019	———	0.24
	25	560.7	-42.6	-64.0	———	0.0264	0.0022	———	0.58
	26	561.2	-41.0	-61.7	———	0.0316	0.0029	———	0.92
	27	561.7	-40.5	-69.4	———	0.0335	0.0012	———	1.25
	28	562.2	-41.0	-68.5	———	0.0316	0.0013	———	1.59
	29	562.7	-43.2	-58.3	———	0.0247	0.0043	———	1.93
	30	563.2	-46.0	-58.8	———	0.0178	0.0041	———	2.27
	31	563.7	-49.0	-58.9	———	0.0126	0.0041	———	2.61
	32	564.2	-51.7	-57.9	———	0.0092	0.0045	———	2.95
	33	564.7	-53.6	-55.9	-69.0	0.0074	0.0057	0.0013	3.29
	34	565.2	-54.4	-53.9	-64.5	0.0068	0.0072	0.0021	3.63
	35	565.7	-53.7	-51.5	-62.4	0.0073	0.0094	0.0027	3.97
	36	566.2	-52.4	-50.0	-61.9	0.-085	0.0085	0.0029	4.30
	37	566.7	-50.6	-50.7	-60.1	0.0105	0.0105	0.0035	4.64
	38	567.2	-49.7	-67.8	-56.0	0.0116	0.0115	0.0056	4.98

mode	time	f_u	f_L	f_r	Q	E
010	41	561.45	558.48	559.96	188.60	0
020	44	1125.52	1120.92	1123.22	243.91	0.29×10^{-2}
030	47	1700.77	1696.08	1698.43	362.29	0.11×10^{-1}
100	50	1144.24	1140.17	1142.21	280.92	0.17×10^{-1}

REFERENCES

1. Coppens, A.B., and Sanders, J.V., "Finite-Amplitude Standing Waves in Rigid Walled Tubes," J. Acoust. Soc. Am., 43, pp. 516-529, March 1968.

2. Coppens, A.B., and Sanders, J.V., "Finite-Amplitude Waves Within Real Cavities," J. Acoust. Soc. Am., 58, pp. 1133-1140, December 1975.

3. Aydin, M., "Theoretical Study of Finite-Amplitude Standing Waves in Rectangular Cavities With Perturbed Boundaries," Thesis, Naval Postgraduate School, Monterey, California, 1978.

4. Coppens, A.B., "Finite Amplitude Standing Waves in Rectangular Cavities With Degeneracies and Weakly-Perturbed Walls," J. Acoust. Soc. Am., 64, Suppl. 1, S34(A), 1978.

5. Kuntsal, E., "Finite Amplitude Standing Waves in Rectangular Cavities with Perturbed Boundaries," Thesis, Naval Postgraduate School, Monterey, California, 1978.

INITIAL DISTRIBUTION LIST

		No. Copies
1.	Defense Technical Information Center Cameron Station Alexandria, VA 22314	2
2.	Library, Code 0142 Naval Postgraduate School Monterey, CA 93940	2
3.	Department Library, Code 61 Department of Physics Naval Postgraduate School Monterey, CA 93940	1
4.	Professor James V. Sanders, Code 61Sd Department of Physics Naval Postgraduate School Monterey, CA 93940	5
5.	Professor Alan B. Coppens, Code 61Cz Department of Physics Naval Postgraduate School Monterey, CA 93940	5
6.	Dr. Logan Hargrove, Code 421 Office of Naval Research 800 Quincy St. Arlington, VA 22217	6
7.	CDR Il Bok Joung 425 Waupelani Dr #207 State College, PA 16801	5


FILMED
7-8